Morphology and Connections of Nucleus Isthmi Pars Magnocellularis in Chicks (*Gallus gallus*)

YUAN WANG, DANIEL E. MAJOR, AND HARVEY J. KARTEN*

Department of Neurosciences, University of California San Diego, La Jolla, California 92093

ABSTRACT

The nucleus isthmi pars magnocellularis (Imc) and pars parvocellularis (Ipc) influence the receptive field structure of neurons in the optic tectum (TeO). To understand better the anatomical substrate of isthmotectal interactions, neuronal morphology and connections of Imc were examined in chicks (*Gallus gallus*). Cholera toxin B injection into TeO demonstrated a coarse topographical projection from TeO upon Imc. Retrogradely labeled neurons were scattered throughout Imc and in low density within the zone of anterogradely labeled terminals, suggesting a heterotopic projection from Imc upon TeO. This organization differed from the precise homotopic reciprocal connections of Ipc and the nucleus isthmi pars semilunaris (SLu) with TeO. By using slice preparations, extracellular biotinylated dextran amine injections demonstrated a dense projection from most neurons in Imc upon both Ipc and SLu. Intracellular filling of Imc neurons with biocytin revealed two cell types. The most common, *Imc-Is,* formed a widely ramifying axonal field in both Ipc and SLu, without obvious topography. A less frequently observed cell type, *Imc-Te,* formed a widely ramifying terminal field in layers 10–12 of TeO. No neurons were found to project upon both Ipc/SLu and TeO. Both types possessed local axon collaterals and flat dendritic fields oriented parallel to the long axis of Imc. Imc neurons contain glutamic acid decarboxylase, which is consistent with Imc participating in center-surround or other wide-field inhibitory isthmotectal interactions. The laminar and columnar pattern of isthmotectal terminals also suggests a means of interacting with multiple tectofugal pathways, including the stratified subpopulations of tectorotundal neurons participating in motion detection. J. Comp. Neurol. 469:275–297, 2004. © 2003 Wiley-Liss, Inc.

Indexing terms: optic tectum; retinotopic; homotopic; heterotopic; center-surround interaction; motion detection

The isthmic complex in birds consists of four cytoarchitectonically distinct midbrain nuclei: the nucleus isthmi pars magnocellularis (Imc), pars parvocellularis (Ipc), and pars semilunaris (SLu) and the nucleus isthmo-opticus (ION; Ariëns Kappers et al., 1960). The ION projects upon the displaced retinal ganglion cells of the accessory optic system (McGill et al., 1966; Uchiyama, 1989; Woodson et al., 1995) and does not appear to play a direct role in the functions of the other isthmic nuclei. Imc, Ipc, and SLu all have reciprocal connections with the ipsilateral optic tectum (TeO; Hunt and Künzle, 1976; Brecha, 1978; Hellmann et al., 2001). Imc and Ipc have been postulated to participate in visual processing interactions with the TeO, such as delayed, prolonged excitations (Sereno and Ulinski, 1987); center-surround interactions (Sereno and Ulinski, 1987; Y. Wang et al., 2000); and construction of a "winner-take-all" network (Sereno and Ulinski, 1987; Wang and Frost, 1991; Wang, 2003).

Imc can be distinguished from Ipc and SLu based on developmental, hodological, and neurochemical features. Both Ipc and SLu originate from the dorsal cell column of

the isthmic migration within the rhombencephalon (Vaage, 1973). They maintain a precise reciprocal retinotopic connection with the TeO (Brecha, 1978; Güntürkün and Remy, 1990; Hellmann et al., 2001). Most of their neurons are cholinergic (Sorenson et al., 1989; Medina and Reiner, 1994; Hellmann et al., 2001). In contrast, Imc originates from the dorsolateral cell column within the mesencephalon (Palmgren, 1921). The organization of Imc-TeO connections remains obscure (Karten, 1967; Hunt and Künzle, 1976; Brecha, 1978). Hodos and Karten (1974) suggested from lesion studies that Imc axons pass through or very close to Ipc, but their termination sites have not been confirmed. The somata of Imc neurons are rich in γ-aminobutyric acid (GABA), and Ipc contains a dense population of GABAergic terminals (Granda and Crossland, 1989; Tömböl et al., 1995). However, the extent and character of the projection from Imc to Ipc are poorly understood. The relationship of SLu to Imc has not been previously examined.

Imc has a narrow configuration and is situated between the overlying TeO and Ipc. Attempts to place tracers into Imc in vivo by using stereotaxic methods are difficult to interpret, insofar as the tracers often spread to these adjacent structures. Furthermore, because fibers passing between the TeO and Ipc pass through Imc itself (Ramón y Cajal, 1911; Hunt and Künzle, 1976; Y. Wang, unpublished observation), fibers of passage confound conventional tracing studies. In contrast, in vitro slice methods allow for precise placement of tracers into a nucleus or intracellularly label individual neurons to demonstrate their projections unambiguously.

Here we describe the morphology and connections of Imc neurons as revealed in three experiments. In the first experiment, the topography of the Imc-TeO projection was clarified by small in vivo injections of cholera toxin B subunit (CTB) into the TeO. In the second experiment, the extents of the Imc-Ipc and Imc-SLu projections were clarified with in vitro placement of biotinylated dextran amine (BDA) into either Imc or Ipc in slice preparations. In the third experiment, the morphology and projections of individual Imc neurons upon Ipc, SLu, and TeO were revealed with in vitro intracellular iontophoretic injections of biocytin. Cytoarchitectonic, histochemical, and immunocytochemical features of the isthmic complex are also described. Details of the Ipc-TeO system will be described in a subsequent report by Luksch et al. (in preparation). The current study identifies anatomical substrates of proposed isthmotectal interactions. Given the columnar and laminar patterns of isthmotectal terminals, interactions with other functional tectofugal systems are also considered.

MATERIALS AND METHODS

This study was performed on 41 white leghorn chick hatchlings (*Gallus gallus*). All procedures used in this study were approved by the University of California, San Diego, Animal Care Committee and conformed to the guidelines of the National Institutes of Health on the Care and Use of Laboratory Animals.

Nissl, histochemical, and immunocytochemical staining

Three chicks under 5 days of age were anesthetized with a mixture of 40 mg/kg ketamine and 12 mg/kg xylazine and transcardially perfused with 0.9% saline, followed by chilled 4% paraformaldehyde in phosphate buffer (PB; 0.1 M; pH 7.2–7.4). The brains were removed from the skull, postfixed overnight in the paraformaldehyde solution, and then transferred to 30% sucrose in PB until they sank, which usually took 3–7 days. Each brain was frozen and cut either horizontally or coronally at 30 μm on a freezing sliding microtome, and each section was collected in phosphate-buffered saline (PBS; 0.1 M; pH 7.2–7.4). Sections from alternate series were stained for Nissl substance or acetylcholinesterase (AChE) histochemistry according to the procedures of Katz and Karten (1983).

Glutamic acid decarboxylase (GAD) was immunocytochemically localized according to the procedures of Mpodozis et al. (1996). Briefly, sections were incubated with monoclonal mouse antibodies against chick GAD-2, (1:2,000; provided by Dr. David Gottlieb, Washington University School of Medicine, St. Louis, MO), followed by biotinylated anti-mouse IgG antibodies (1:200; Vector Laboratories, Burlingame, CA). Sections were then incubated in avidin-biotin-peroxidase complex solution (ABC Elite Kit; Vector Laboratories) diluted 1:200 in PBS with 0.3% Triton X-100 for 1 hour at room temperature. Sections were incubated for 5–7 minutes in 0.025% 3-3′-diaminobenzidine (DAB; Sigma, St. Louis, MO) with 0.01% hydrogen peroxide in PB. Sections were mounted on gelatin-coated slides and stained with 0.05% osmium tetroxide for 30 seconds. Sections were then dehydrated, cleared, and coverslipped with Permount (Fisher Scientific, Pittsburgh, PA).

CTB injections into the TeO in vivo

Eight chicks under 5 days of age were anesthetized as described above and placed in a stereotaxic head holder. The skull was exposed, and a hole was made above the TeO. A solution of 1% CTB (List Laboratories, Campbell, CA) in PB was injected through a glass micropipette by using a pressure device (PicoSpritzer II; General Valve, Fairfield, NJ). The micropipette was retracted, the wound was closed, and the animal was allowed to recover. After a survival time of 3–5 days, animals were anesthetized with ketamine and xylazine and perfused with paraformaldehyde solution as described above. The brains were removed from the skull, postfixed, equilibrated in sucrose, and sectioned at 30 μm as described above. Standard immunohistochemistry procedures were applied to reveal CTB distribution (see Shimizu et al., 1994; Rodman and Karten, 1995). Briefly, sections were incubated with antibodies against CTB made in goat (1:12,000; List Laboratories), followed by biotinylated anti-goat IgG antibodies (1:200; Vector Laboratories). ABC complex solution and DAB were used as the final steps in visualization of CTB. Sections were mounted on gelatin-coated slides and were either stained with 0.05% osmium tetroxide for 30 seconds or counterstained with Giemsa (Iñiguez et al., 1985). Sections were then dehydrated, cleared, and coverslipped with Permount (Fisher Scientific).

BDA injections and intracellular filling in vitro

Thirty chicks under 3 days of age were anesthetized as described above and then decapitated. The brains were quickly removed from the skull and placed in a dish of chilled, oxygenated, and sucrose-substituted artificial cerebrospinal fluid (ACSF; 240 mM sucrose, 3 mM KCl, 3

mM MgCl$_2$, 23 mM NaHCO$_3$, 1.2 mM NaH$_2$PO$_4$, 11 mM D-glucose). The midbrain was blocked and sectioned at 500 μm on a Vibroslice (Campden Vibroslice; World Precision Instruments, Sarasota, FL) in either the horizontal or the coronal plane. For sagittal slices, the tectal hemispheres were separated with a midsagittal cut and sectioned separately at 500 μm. Slices were collected and submerged in a collecting chamber containing ACSF (119 mM NaCl, 2.5 mM KCl, 1.3 mM Mg$_2$SO$_4$, 1.0 mM NaH$_2$PO$_4$, 26.2 mM NaHCO$_3$, 11 mM D-glucose, 2.5 mM CaCl$_2$) at room temperature and continuously oxygenated with carbogen (95% O$_2$, 5% CO$_2$).

Prior to injection of BDA, the slices were transferred to a dish mounted on a stereo dissecting microscope (Wild Heerbrugg). The surface of the tissue was briefly dried with low-pressure carbogen blown through a syringe. One preparation or a few penetrations through the tissue in either Imc or Ipc were made, by using a metal needle whose tip was covered with BDA crystals (10,000 molecular weight; Molecular Probes, Eugene, OR). Then, the slices were quickly transferred back to the collecting chamber. Drying and injecting of the slice took less than 30 seconds. The slices were kept in oxygenated ACSF for an additional 6 hours before fixation.

The slices for intracellular filling were transferred to a chamber (model RC-27L Large Bath Chamber; Warner Instrument, Inc., Hamden, CT) mounted on an upright, fixed-stage microscope (Laborlux FS-12; Leitz, Wetzlar, Germany) equipped with fluorescent optics and Nikon long-working-distance objectives (×4, 10 mm W.D.; ×10, 10 mm W.D.). The chamber was perfused continuously with oxygenated ACSF at room temperature. A recording electrode (100–300 MΩ) was prepared on a micropipette puller (model P80/PC; Sutter Instrument Company, Novato, CA) and filled with 4% biocytin (Sigma) and 1% fluorescent pyranine (Molecular Probes) in 0.3 M KAc (pH 7.2–7.8). The electrode was positioned over Imc with a micromanipulator and advanced through the tissue with a single-axis hydraulic drive (Newport Corp., Irvine, CA). The addition of pyranine to the recording solution was used to visualize the electrode without changing the electrode characteristics. Cell penetration was indicated by a sudden negative voltage drop and cell discharges. If the membrane potential of a neuron remained stable at more than –30 mV, biocytin was iontophoresed into the neuron with the iontophoresis unit of an intracellular amplifier (AM Systems, Everett, WA). Injection parameters were usually 2–3 nA of positive current for 2–3 minutes. After injection of only one cell in a single slice, slices were kept in oxygenated ACSF for an additional 30 minutes.

All slices were subsequently fixed by immersion in 4% paraformaldehyde in PB overnight and then transferred to 30% sucrose in PB until they sank, which usually took 1–2 days. Each slice was frozen and resectioned at 80 μm on the freezing sliding microtome. Sections were collected in PBS, kept for 10 minutes in 0.6% hydrogen peroxide in methanol to block endogenous peroxidase activity, and washed again in PBS. Sections were then incubated in ABC complex solution at 4°C overnight. The reaction product was visualized with DAB. Sections were mounted on gelatin-coated slides and immersed in 0.05% osmium tetroxide for 30 seconds to enhance the DAB reaction product. Sections were then dehydrated, cleared, and coverslipped with Permount (Fisher Scientific). Counter-

staining was avoided so as not to obscure fine cellular processes.

Imaging and cell reconstruction

All CTB-labeled neurons and terminals and all intracellularly filled neurons were reconstructed with a camera lucida on a Zeiss WL microscope (Carl Zeiss, Inc., Thornwood, NY). The drawings were then digitized and edited in Canvas (Deneba Systems, Miami, FL). Digital images of selected sections and cells were captured with a Nikon D100 digital camera mounted on a Nikon photomicroscope (Nikon Corp., Tokyo, Japan). Image contrast adjustments and photomontages were made in Adobe Photoshop (Adobe Systems Inc., Mountain View, CA). Measurements of dendritic field dimensions were based on the cell reconstructions. Measurements of soma size and dendritic caliber were made on both cell reconstructions and calibrated images captured with a BW CCD camera, using the public domain NIH Image program. The measurements with the two methods were consistent with each other. No corrections were made for tissue shrinkage.

Camera-lucida reconstructions generate two-dimensional projections of three-dimensional objects and so introduce artifacts relevant to the current study. First, the relative positions of structural boundaries change significantly in two-dimensional projections of volumes in 500-μm-thick slices. Second, slice preparations that do not capture the full axonal or dendritic field of a cell prevent many higher order branches in the slice from being labeled when low-order branches pass out of the slice volume (see Major et al., 2000). Both artifacts can be minimized by only reconstructing structures within a volume significantly smaller than the slice itself. In the case of the high-density axonal arborizations filling Ipc and SLu, axons from three adjacent 80-μm-thick sections (i.e., 240 μm of a 500-μm slice) that contained the soma were reconstructed. Dendrites and the axon branches within the TeO were reconstructed from all sections; they were relatively sparse.

RESULTS
Nissl, histochemical, and immunocytochemical staining

Figure 1A and B demonstrates the general cytoarchitecture and AChE histochemical staining, respectively, of Imc, Ipc, and SLu. Imc is lenticular in shape, lies deep to the stratum album centrale (SAC) of the TeO, and is directly lateral to the brachium colliculi superioris (BCS). Imc is composed of loosely packed stellate cells 10–50 μm in diameter. Ipc is the largest subdivision of the isthmic complex and is located dorsomedially to Imc and ventrally to the nucleus mesencephalicus lateralis pars dorsalis (MLd). SLu is the smallest subdivision and is located medially and caudally to Imc and Ipc. Both Ipc and SLu are composed of closely packed round or oval cells about 20 μm in diameter, and show distinct boundaries. On AChE histochemical staining (Fig. 1B), both neuropil and cells within Imc, Ipc, and SLu are darkly stained, whereas the BCS and SAC are lightly stained with a few positive fibers.

A bundle of fibers extends from the rostrolateral gap between Imc and Ipc to the caudolateral edge of SLu (arrowheads, Fig. 1A). This bundle will be referred to as the *tractus intraisthmicus* (Tii). Showers and Lyons (1968) mentioned the existence of the fibers between
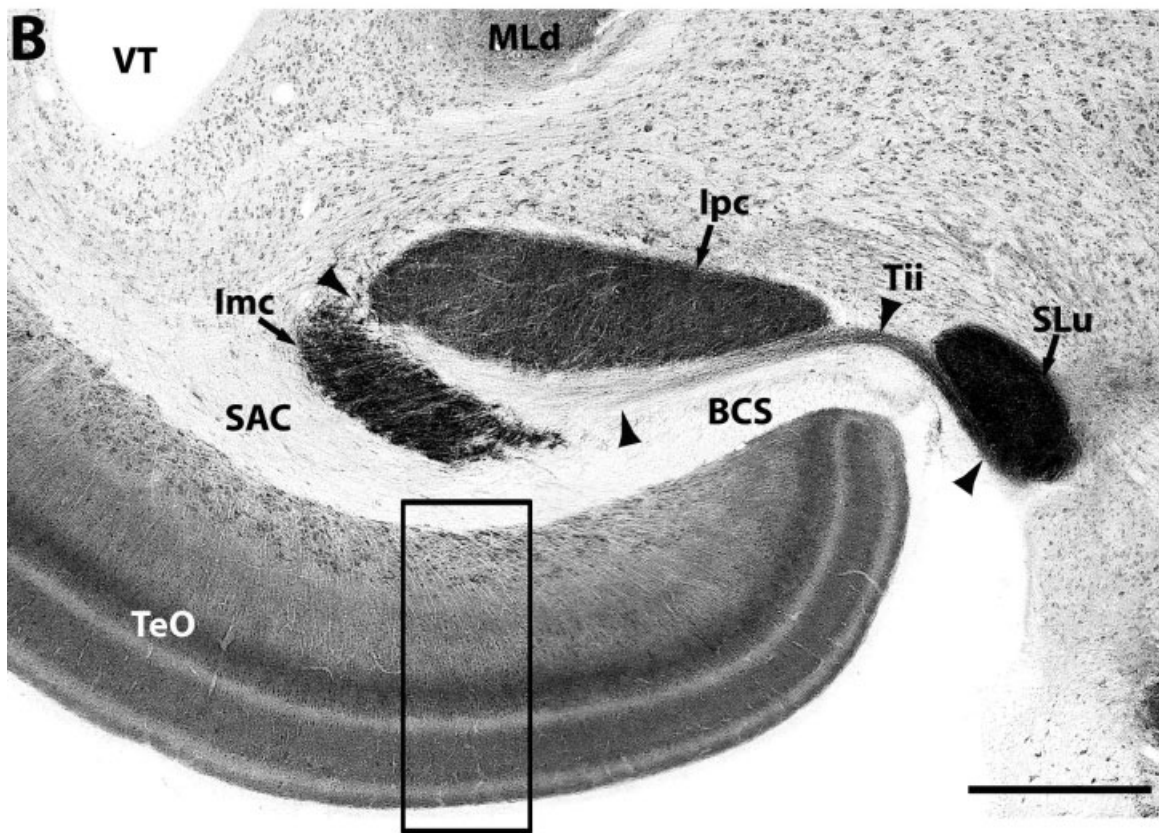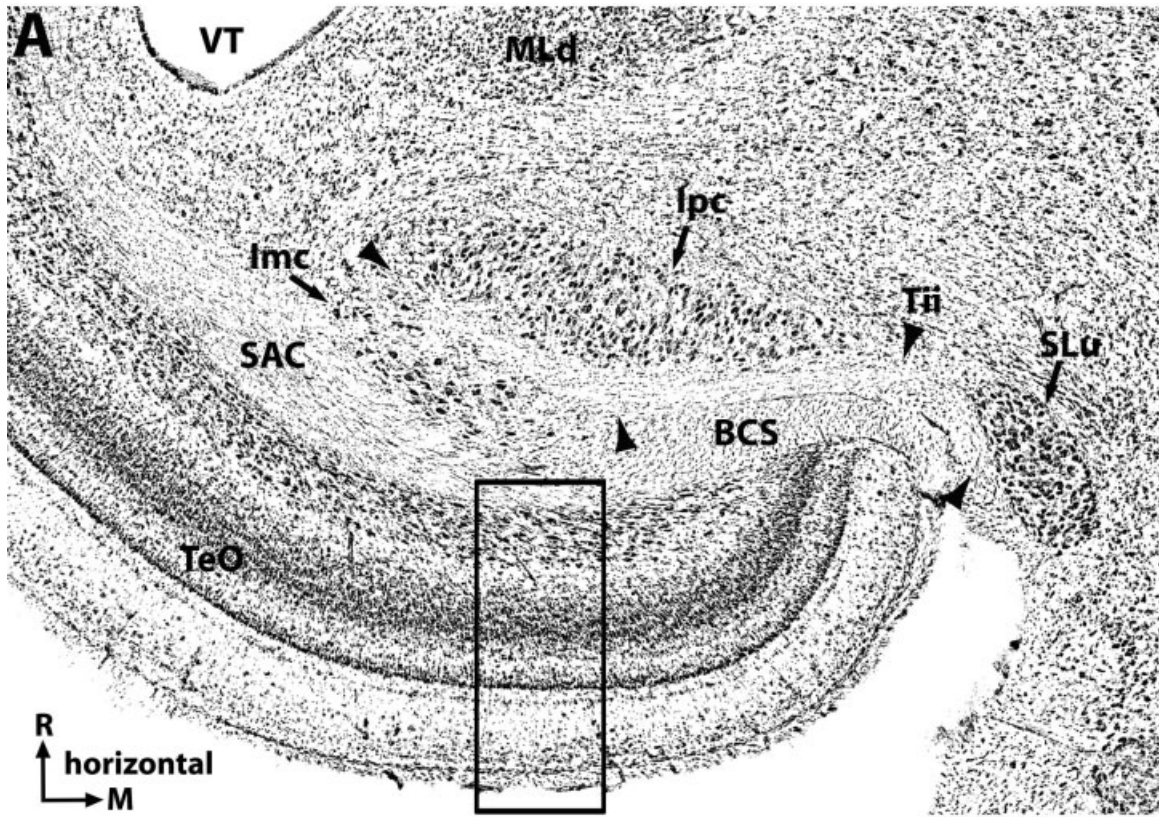
Fig. 1. Nissl (**A**) and AChE histochemical (**B**) staining of Imc, Ipc, and SLu in the horizontal plane. Arrowheads indicate the course of the Tii. VT, ventriculus tecti mesencephali; MLd, nucleus mesencephalicus lateralis pars dorsalis; Imc, nucleus isthmi pars magnocellularis; Ipc, nucleus isthmi pars parvocellularis; SLu, nucleus isthmi pars semilunaris; Tii, tractus intraisthmicus; SAC, stratum album centrale; BCS, brachium colliculi superioris; TeO, optic tectum. Boxed areas are shown at higher magnification in Figure 2. Scale bar = 500 μm.
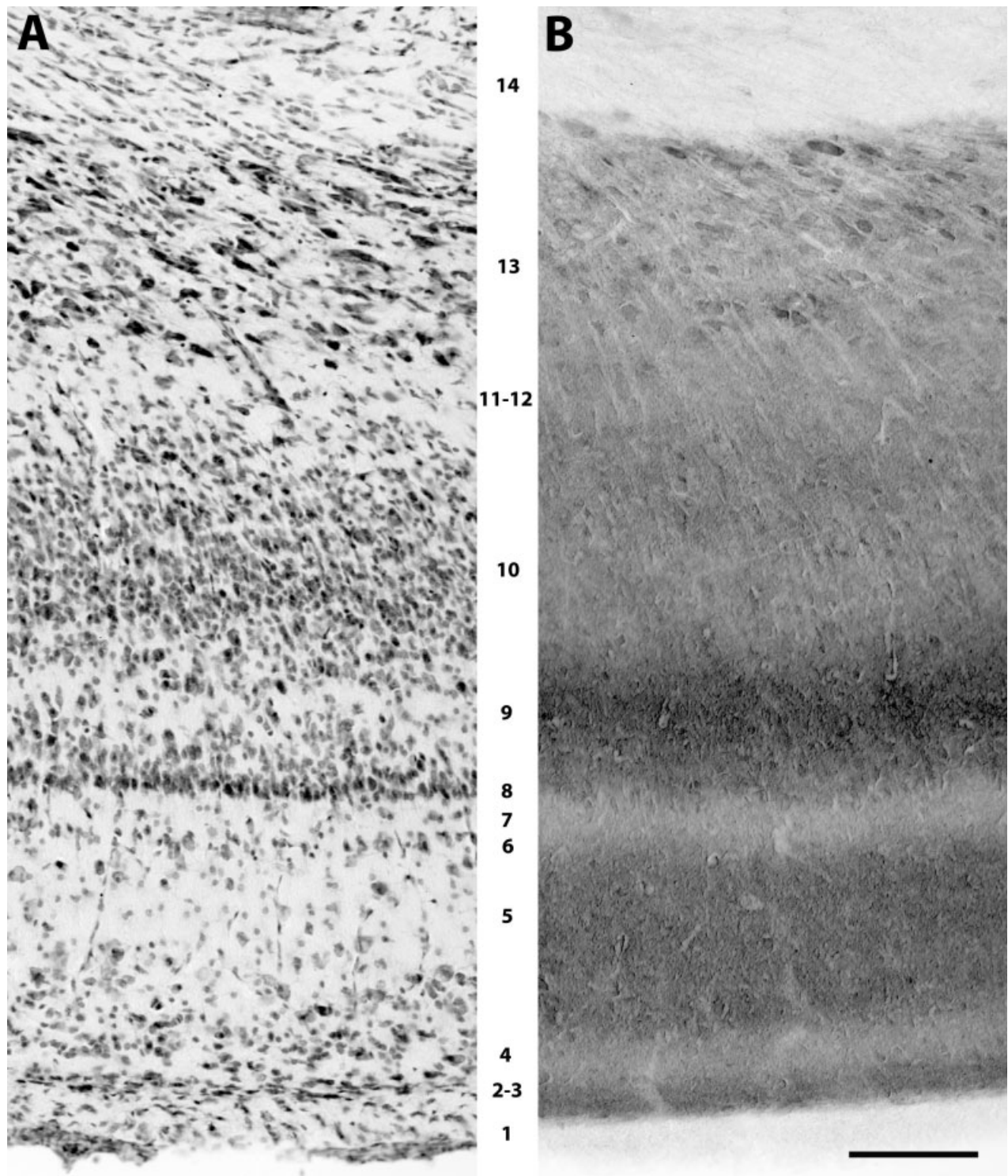
Fig. 2.   Nissl (**A**) and AChE histochemical (**B**) staining of the caudomedial TeO in the horizontal plane from the areas in the corresponding boxes in Figure 1A and B. Numbers indicate tectal layers according to the nomenclature of Ramón y Cajal (1911). Scale bar = 50 μm.

Imc and Ipc that may constitute the whole or a component of the Tii. AChE histochemical staining shows that the Tii contains a prominent bundle of darkly staining fibers (arrowheads, Fig. 1B). Sorenson et al. (1989) did not visualize the Tii on ChAT immunohistochemical staining.
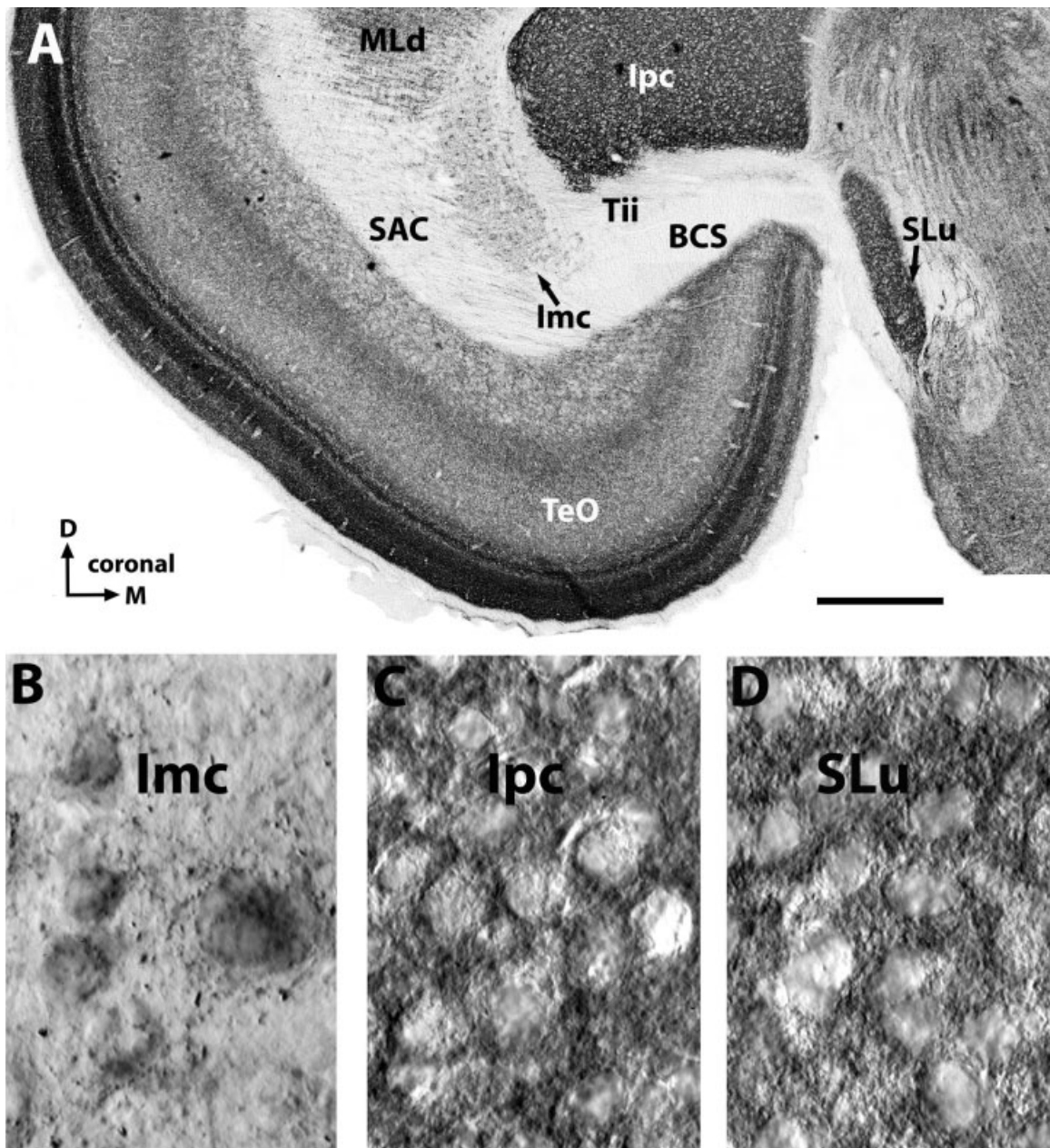
Fig. 3. GAD immunocytochemical staining of the ventrocaudal TeO (**A**), Imc (**B**), Ipc (**C**), and SLu (**D**) in the coronal plane. A is a low-magnification photomontage. B–D are high-magnification Nomarski-DIC photomicrographs. Scale bar = 500 μm for A; 30 μm for B–D.

Figure 2A and B demonstrates the laminated cytoarchitecture and AChE histochemical staining, respectively, of the caudomedial TeO. The alternating cell and fiber layers of the TeO are numbered according to the nomenclature of Ramón y Cajal (1911). Layer 14 is the SAC, and layer 1 is the stratum opticum (SO), both of which are lightly stained for AChE and contain very finely labeled fibers. Labeled fibers are found in all other tectal layers, with the darkest staining in layers 2–3, 5, and 9. The large cells of layer 13, the stratum griseum central (SGC), are conspicuously labeled as

against relatively light labeling in the surround neuropil.

Figure 3 demonstrates the GAD immunocytochemical staining of Imc, Ipc, SLu, and ventrocaudal TeO. Many Imc neurons exhibit light staining for GAD (Fig. 3A) and are surrounded by perisomatic clusters of GAD-immunoreactive terminal boutons (Fig. 3B). The neuropils in Ipc and SLu are intensely stained for GAD, but none of the somata of Ipc and SLu neurons are GAD immunoreactive (Fig. 3C,D). Some fibers in the Tii are GAD immunoreactive (Fig. 3A). In the TeO, the neuropil and a few
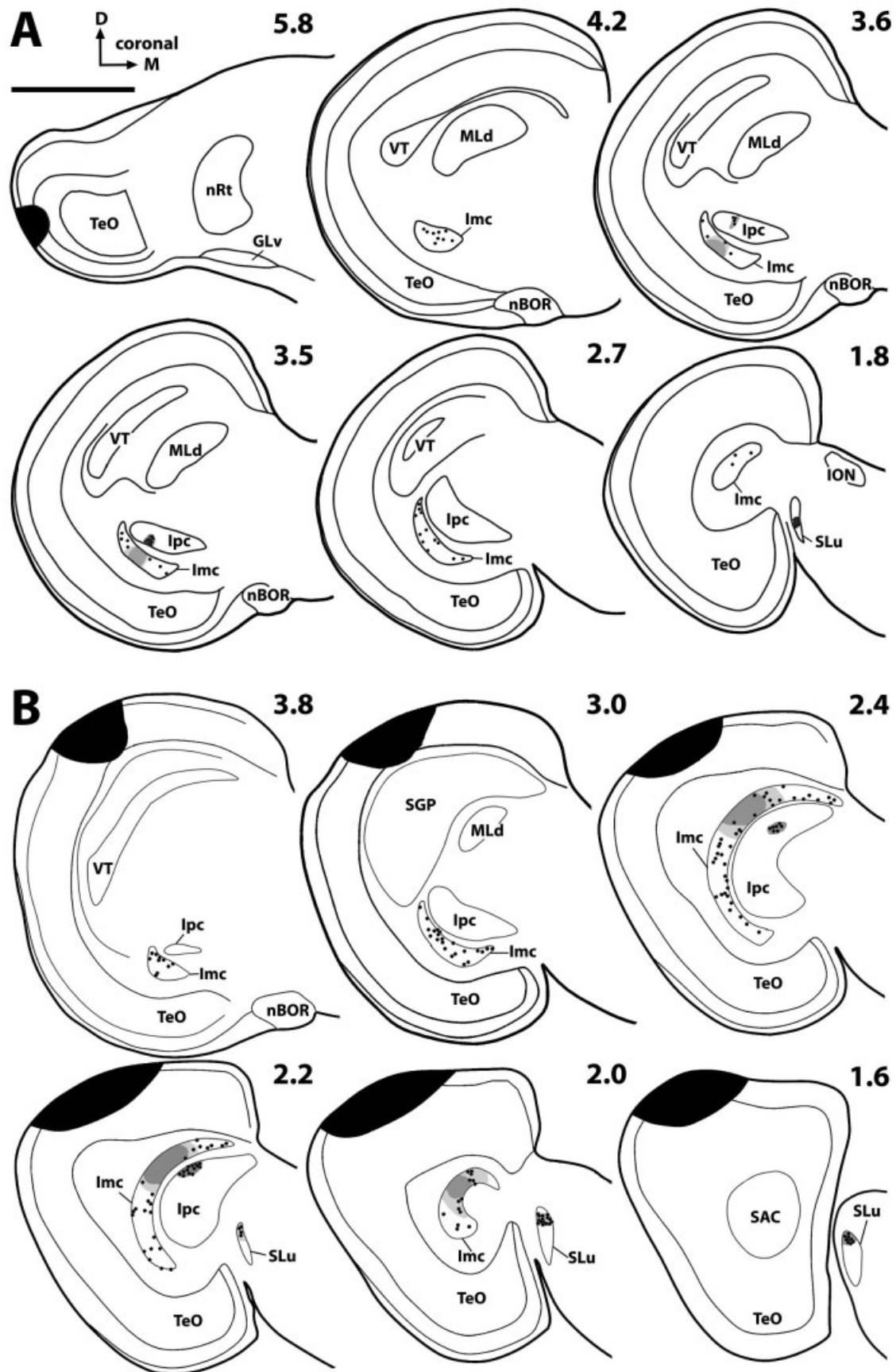
Fig. 4. Line drawings illustrating the distribution of retrogradely labeled neurons and anterogradely labeled tectal terminal fields within Imc, Ipc, and SLu after a CTB injection into the rostrolateral (**A**) or dorsocaudal (**B**) TeO. Black areas indicate injection sites. Each circle represents a single labeled neuron. Darkly and lightly shaded areas represent the primary and peripheral zones of tectal terminal fields, respectively. Approximate anterior-posterior stereotaxic levels are indicated at upper right in each drawing. nBOR, nucleus of the basal optic root; ION, nucleus isthmoopticus; nRt, nucleus rotundus; GLv, nucleus geniculatus lateralis pars ventralis. For other abbreviations see Figure 1 legend. Scale bar = 1 mm.

scattered cells in layers 2–7 exhibit intense GAD immunoreactivity (Fig. 3A).

CTB injections into the TeO

The topography of the Imc-TeO projection was clarified by in vivo injections of CTB into the dorsocaudal (five cases), caudolateral (one case), or rostrolateral (two cases) TeO. Injections into the ventral TeO were not attempted because of the probable spread of tracer directly into Imc or Ipc. There is widespread anterograde and retrograde labeling after tectal injections, but the current study focuses on Imc, Ipc, and SLu. Injections in the rostral (Fig. 4A) or caudal (Fig. 4B) portions of the TeO resulted in anterograde terminal label in the rostral or caudal portions, respectively, of Imc, Ipc, and SLu. Retrogradely labeled cells were found within the zone of anterograde terminal label in Ipc and SLu. In contrast, within Imc, retrogradely labeled neurons were scattered throughout the nucleus (Fig. 5C) and at notably low density within the zone of anterograde terminal label (Fig. 5A,B). To determine whether Imc neurons project back upon their tectal input region, small injections were placed in the TeO to investigate the more detailed topography of connections between Imc and the TeO.

Figure 6 illustrates a small injection in the dorsocaudal TeO without apparent spread into layer 13 or below (Fig. 7A). Within Ipc and SLu, the anterogradely labeled terminals were sharply limited in distribution and found in the caudal sections of these nuclei (Fig. 7B,E). Each retrogradely labeled Ipc and SLu neuron was surrounded by labeled tectal terminals and covered with a high density of boutons (Fig. 7C,F). The anterogradely labeled terminals in Imc, also found in the same caudal sections as Ipc, formed a diffuse and relatively larger field compared with that in Ipc and SLu (Fig. 7B). No Imc neurons were retrogradely labeled within this tectal projection zone. Figure 7G shows an unstained Imc neuron that was surrounded by dense labeled tectal terminals with boutons. In contrast, retrogradely labeled Imc neurons were widely scattered within other portions of Imc. None of the somata of these labeled Imc neurons appeared to be contacted by labeled tectal terminals under high-power Nomarski-DIC observation. As dendrites of Imc neurons were not labeled in their entirety, we cannot definitely state whether the dendrites of labeled Imc neurons receive synaptic input from tectal fibers. Some thick-caliber tectal fibers passed by some medially situated Imc neurons in their course to the BCS but did not emit collateral arbors upon Imc neurons (Fig. 7D).

BDA injections into Ipc and into Imc

Repeated attempts to place tracer into Imc in vivo without it spreading into Ipc and TeO were unsuccessful. The extent of the Imc-Ipc and Imc-SLu projections were then clarified with in vitro placement of BDA into either Imc or Ipc in slice preparations.

Injections into Ipc. Small BDA injections into Ipc retrogradely labeled many neurons throughout Imc (Fig. 8A), suggesting a widespread projection from large areas of Imc upon Ipc. The retrogradely labeled neurons had multipolar somata 10–40 μm in diameter. The peripherally situated neurons gave off primary dendrites extending along the margin of the nucleus (arrow, Fig. 8B), whereas the neurons in the center of the nucleus gave off primary dendrites without preferred orientation. Thick
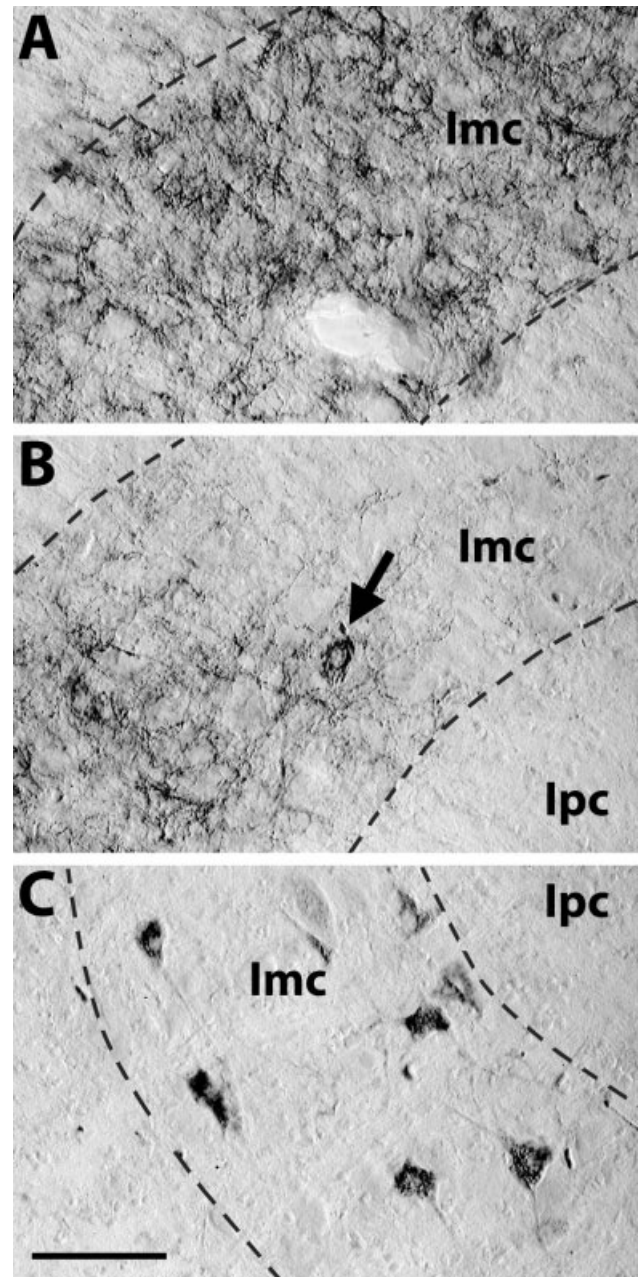

Fig. 5. Nomarski-DIC photomicrographs of anterogradely labeled tectal terminals and retrogradely labeled Imc neurons following the CTB injection into the TeO charted in Figure 4B. **A:** Dense, primary terminal label without labeled neurons. **B:** Sparse, peripheral terminal label with a labeled neuron (arrow) **C:** Most labeled neurons are located outside the zone of terminal label. Scale bar = 200 μm.

axons of Imc neurons could be traced anterogradely into the Tii as far as SLu (black arrow, Fig. 8A). Along the course of the Tii, some axon collaterals entered Ipc and SLu where no labeled neurons were found.

Another bundle of fibers coursed toward the TeO (arrowhead, Fig. 8A). Within the TeO, most retrogradely labeled neurons were bipolar radial neurons situated in layers 10–11. Their dendrites arborized most densely
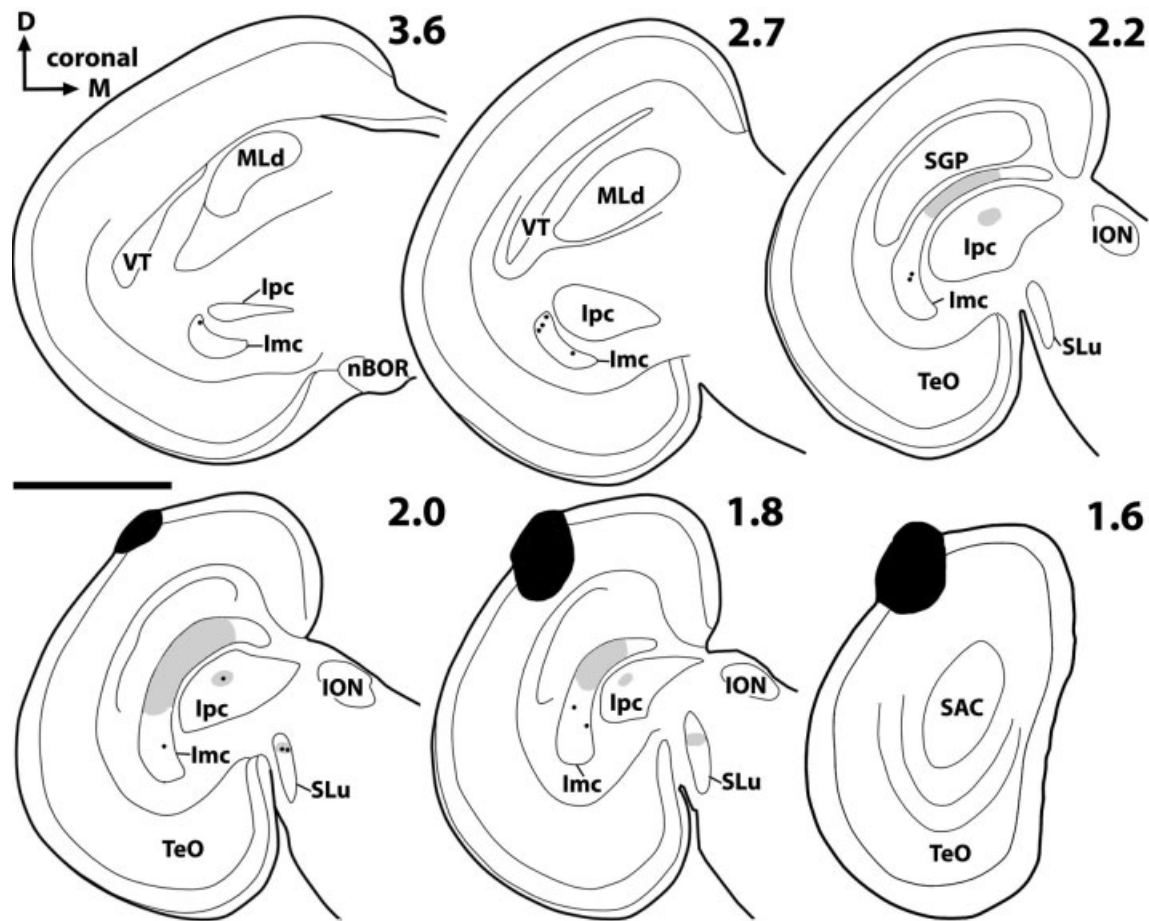
Fig. 6. Line drawings illustrating the distribution of retrogradely labeled neurons and anterogradely labeled tectal terminal fields within Imc, Ipc, and SLu after a small CTB injection into the dorsocaudal TeO. For abbreviations see legends to Figures 1 and 4. Scale bar = 1 mm.

within layers 5, 9, and 11, and their axons arose from primary apical dendritic segments in a classic "shepherd's crook" shape (see Ramón y Cajal, 1911; Domesick and Morest, 1977). Anterogradely labeled arborizations of Ipc displayed 50-μm-wide terminal arborizations extending from layers 2–7 or from 2–10 with sparse branching in layer 8 (for further details see Luksch et al., in preparation). These terminal morphologies are consistent with the "paintbrush" endings described by Ramón y Cajal (1911: Fig. 139).

Injections into Imc. BDA injections into Imc further confirmed the projections from Imc upon Ipc and SLu. Anterogradely labeled Imc axons extended into the Tii, with many collaterals entering Ipc and SLu. None of the Ipc and SLu neurons was labeled, indicating that the connection of Imc with Ipc and SLu is not reciprocal.

Within the TeO, most retrogradely labeled neurons were bipolar radial neurons in layers 10–11 that were similar to the neurons labeled with injections into Ipc. A few paintbrush endings were also intermingled among the apical dendrites of radial tectal neurons. Such neurons and axons could have been labeled by uptake from fibers passing through Imc to the TeO or Ipc. However, some very fine anterogradely labeled ramifications could be dis-

cerned within layers 12–13 that were not labeled with injections into Ipc.

Intracellular filling of Imc neurons

Anterograde and retrograde tracing studies either in vivo or in vitro clarified the reciprocal connection of Imc with the TeO and verified the presence of Imc-Ipc and Imc-SLu projections. The scattered distribution of retrogradely labeled Imc neurons following tracer injections both into TeO and into Ipc suggests that the projections from Imc upon the TeO and Ipc are widely distributed. To describe better the morphology of Imc neurons and their axon terminals, single neurons were intracellularly filled in slice preparations.

Somatodendritic morphology of Imc neurons. Fifty-three Imc neurons were intracellularly labeled. They displayed multipolar somata 10–50 μm in diameter that issued four to eight primary dendrites without preferred orientation. The primary dendritic trunks were 1–5 μm in diameter and tapered with distance. The primary and distal dendrites were up to 400 μm in length and were covered by small filiform spines. Higher order dendrites formed a flat dendritic field 60–400 μm wide by 200–700 μm long oriented parallel to the long axis of Imc. The long
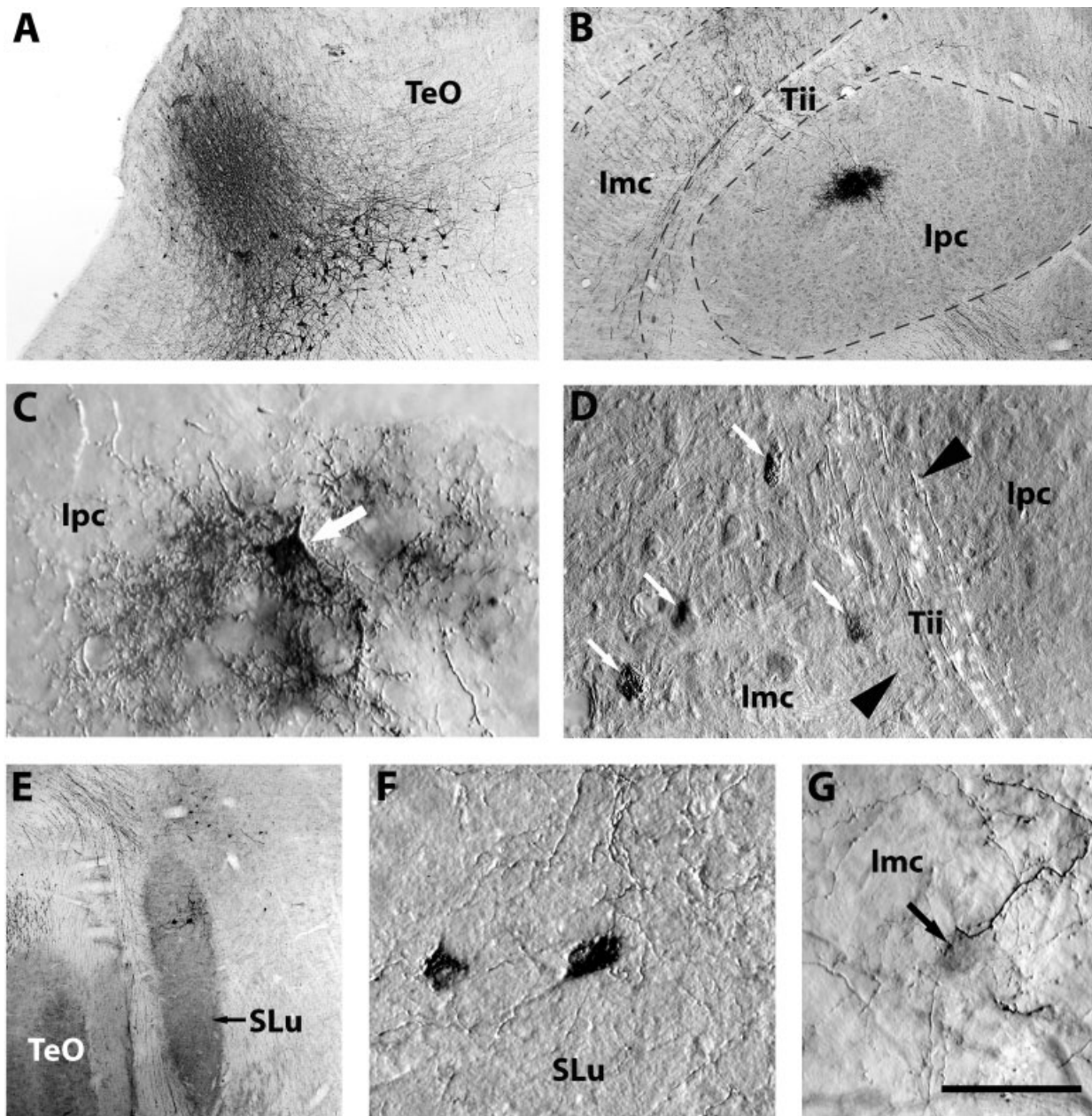
Fig. 7. Brightfield photomicrographs of anterogradely labeled tectal terminals and retrogradely labeled neurons in Imc, Ipc, and SLu following the CTB injection into the TeO charted in Figure 6. **A:** Injection site in superficial layers of the TeO. Labeled multipolar cells are SGC neurons in layer 13. **B:** Small and confined tectal terminal nest in Ipc and larger, less dense tectal terminal field in Imc. **C:** A labeled Ipc neuron (arrow) surrounded by labeled tectal terminals laden with many boutons. **D:** Labeled Imc neurons (arrows). They are not in receipt of labeled tectal terminals. A bundle of thick fibers (arrowheads) traveling between Imc and Ipc does not emit collateral arbors upon Imc neurons. **E:** Anterograde and retrograde labels in SLu. **F:** Labeled SLu neurons that are located within labeled tectal terminals. **G:** An unstained Imc neuron (arrow) situated within labeled tectal terminals. C–D and F–G are high-magnification Nomarski-DIC images. Scale bar = 50 μm in G (applies to C,F,G); 500 μm for A,B,E; 100 μm for D.

axis of Imc is oriented from dorsorostrolaterally to ventrocaudomedially.

Figure 9 is a montage illustrating the somata and dendrites of 13 intracellularly filled Imc neurons in the horizontal plane. Soma size varied widely, and dendrites were generally confined to the nucleus. Peripheral neurons extended their dendrites inward (see Fig. 13) or along the margin of Imc (see Figs. 11A, 12A). More centrally situated neurons displayed fine dendritic arborizations along the margin of Imc (see Figs. 10A–C, 11C).

Axons of Imc neurons. Of the 53 neurons labeled, 28 projected upon Ipc, 3 projected upon both Ipc and SLu, and 15 projected upon the TeO. Seven neurons extended their proximal axons beyond the parent slice, and their termi-
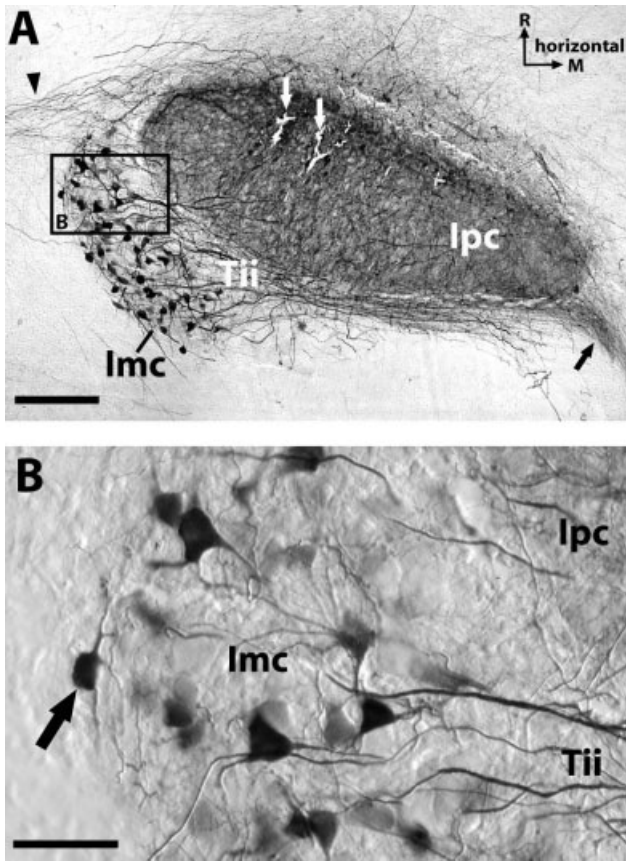
Fig. 8. Photomicrographs in the horizontal plane of retrogradely labeled Imc neurons following BDA injections into Ipc. **A:** Low-magnification image illustrating the multiple injection sites in Ipc (white arrows) and retrogradely labeled Imc neurons throughout the nucleus. The anterogradely labeled Imc fibers extend to Ipc and SLu as the Tii (black arrow). A bundle of fibers courses toward the TeO (arrowhead). **B:** High-magnification Nomarski-DIC image corresponding to the boxed area in A, illustrating labeled Imc neurons. Scale bars = 250 μm in A, 50 μm in B.

Fig. 9. Camera lucida reconstructions of the somata and dendrites of 13 intracellularly filled Imc neurons in the horizontal plane. Scale bar = 100 μm.

nal targets could not be confirmed. Among the 15 neurons projecting to the TeO, 5 gave off axon collaterals that passed through or very close to Ipc toward an unknown target.

Projections upon Ipc and SLu. Figure 10A illustrates an Imc neuron projecting upon Ipc within a horizontal slice. The primary axon emerged from the medial side of the soma (arrow, Fig. 10A,A1) and coursed directly into the Tii after giving off a small collateral arborization within Imc (Fig. 10A2). Every 50–150 μm, the primary axon gave off nearly perpendicular collaterals that extended through Ipc (Fig. 10A3). Intermediate-order collaterals within Ipc tended to course parallel or perpendicular to the boundaries of Ipc. Within Ipc, terminals surrounded the somata of Ipc neurons (Fig. 10A4). The distal axonal branches within Ipc had a high density of boutons, whereas the primary axon within the Tii appeared relatively smooth. The primary axon passed out of the parent slice medially in the Tii.

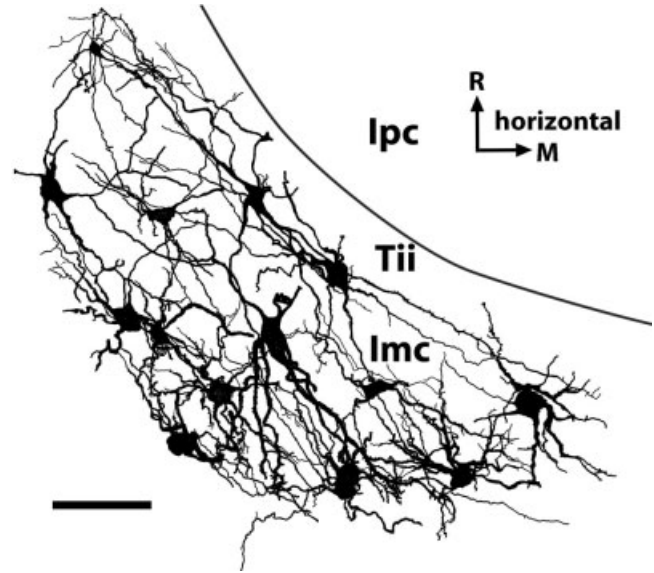In three cases, the primary axons could be followed medially and caudally into SLu. Figure 10B illustrates an

Imc neuron with a small local axonal arborization (arrowhead, Fig. 10B) and an extensive collateralization throughout both Ipc (Fig. 10B1) and SLu (Fig. 10B2). Figure 10C illustrates a comparable neuron, although portions of the axon were lost during tissue processing. The terminals in SLu are comparable to those in Ipc. These particular neurons also display a single axon branch outside of Ipc leaving the slice plane rostromedially (open arrows, Fig. 10B,C).

Similarly to horizontally sectioned neurons, coronally or sagittally sectioned neurons possess extensive arborizations within Ipc (Fig. 10D,E), suggesting that individual Imc neurons project upon the whole volume of Ipc without distinct retinotopy. As SLu was located caudally and medially to Imc and Ipc, it was not visualized with Imc and Ipc in coronal or sagittal slices. Whether the axonal arborizations of individual Imc neurons filled the whole volume of SLu could not be determined.

Projection upon the TeO. Projections upon the TeO consisted of widely branching fine-caliber axons. Figure 11A illustrates an Imc neuron projecting upon the TeO within a horizontal slice. The primary axon coursed along layer 14 (SAC), issuing fine collateral branches that were labeled up to 200 μm before disappearing. Figure 11B illustrates an Imc neuron within a sagittal slice whose axon began ramifying through layer 14 and formed a wide terminal field more than 1,300 μm wide in layers 10–12 (Fig. 11B1). Terminal arbors in layers 10–12 displayed many boutons (Fig. 11B2). More superficial terminals could not be confirmed; the fine-caliber fibers in layer 10 generally faded away as they ascended. Figure 11C is a similar neuron in a horizontal slice. In addition to axonal terminals within the TeO, this neuron gave off a wide local axonal arborization within Imc (open arrow, Fig. 11C) and collaterals extending rostrally or laterally beyond Imc (solid arrows, Fig. 11C).

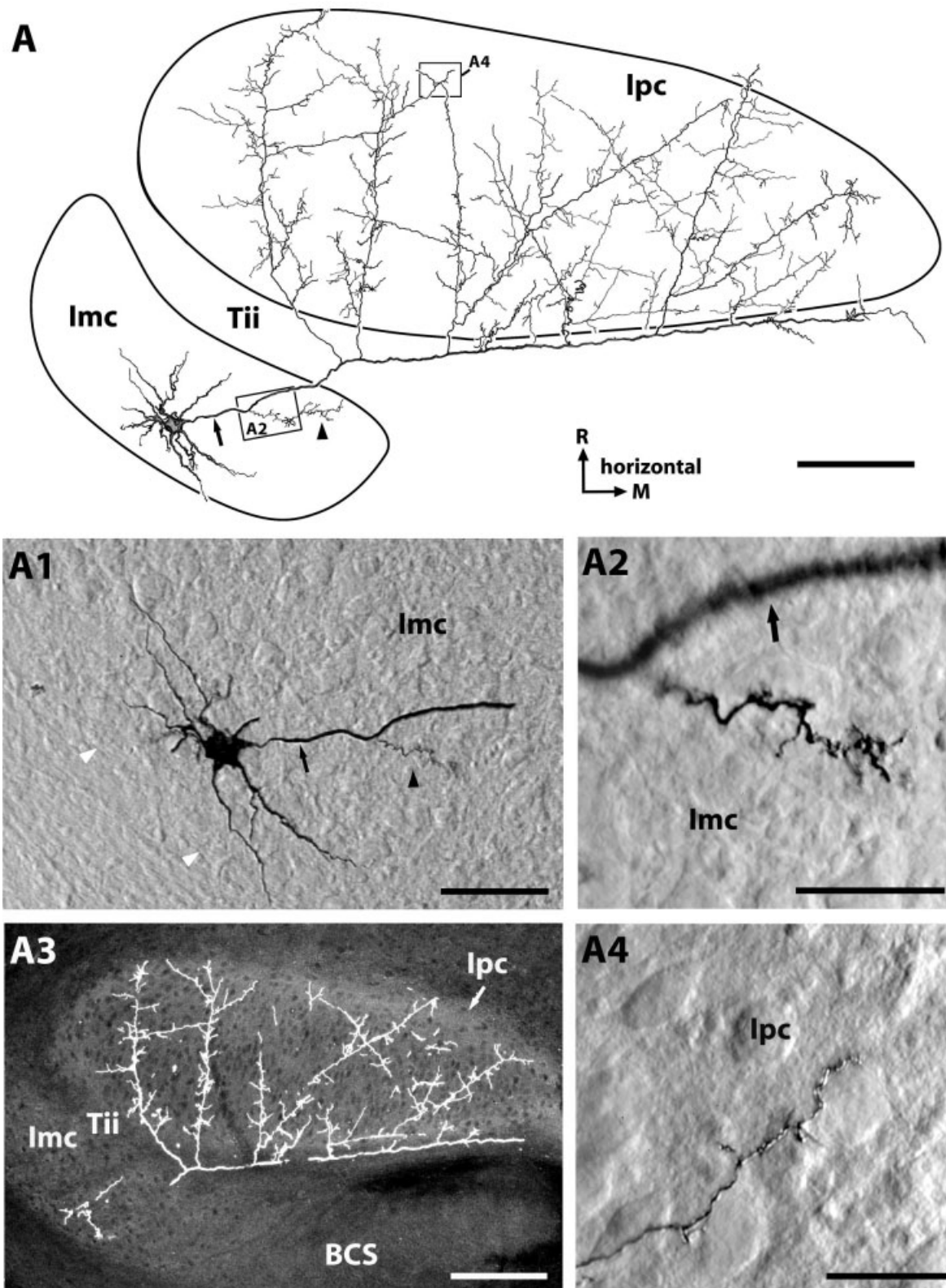*Projection upon unknown targets.* In some cases, axons extended beyond the parent slice before reaching their

Fig. 10. (Continued)Camera lucida reconstructions and photomicrographs of Imc neurons projecting upon Ipc or both Ipc and SLu. The solid arrow indicates the primary axon. **A:** A horizontally sectioned Imc neuron widely projecting upon Ipc. A small, local axonal arborization (arrowhead) is located within Imc and is depicted in A2. **A1:** Nomarski-DIC image of the soma and dendrites. Arrowheads indicate the lateral boundary of Imc. **A2:** High-magnification Nomarski-DIC image of the local arborization. **A3:** Darkfield image of extensive axonal arborization within Ipc. **A4:** A distal terminal arbor of the Imc neuron that surrounds several local Ipc neurons. **B:** A horizontally sectioned Imc neuron projecting upon both Ipc and SLu. A branch (open arrow) extends beyond Ipc rostrally to an unknown target. **B1:** Darkfield image of the section containing the soma and some portions of axonal arborization within Ipc. **B2:** Darkfield image of the section containing axonal arborization within SLu. **C:** A horizontally sectioned Imc neuron projecting upon both Ipc and SLu. Another collateral (open arrow) courses rostrally between Ipc and SLu toward an unknown target. **D:** A coronally sectioned Imc neuron widely projecting upon Ipc. **E:** A sagittally sectioned Imc neuron widely projecting upon Ipc. Scale bars = 200 μm in A,A3,B,B1,B2,C–E; 50 μm in A1,A2; 25 μm in A4.
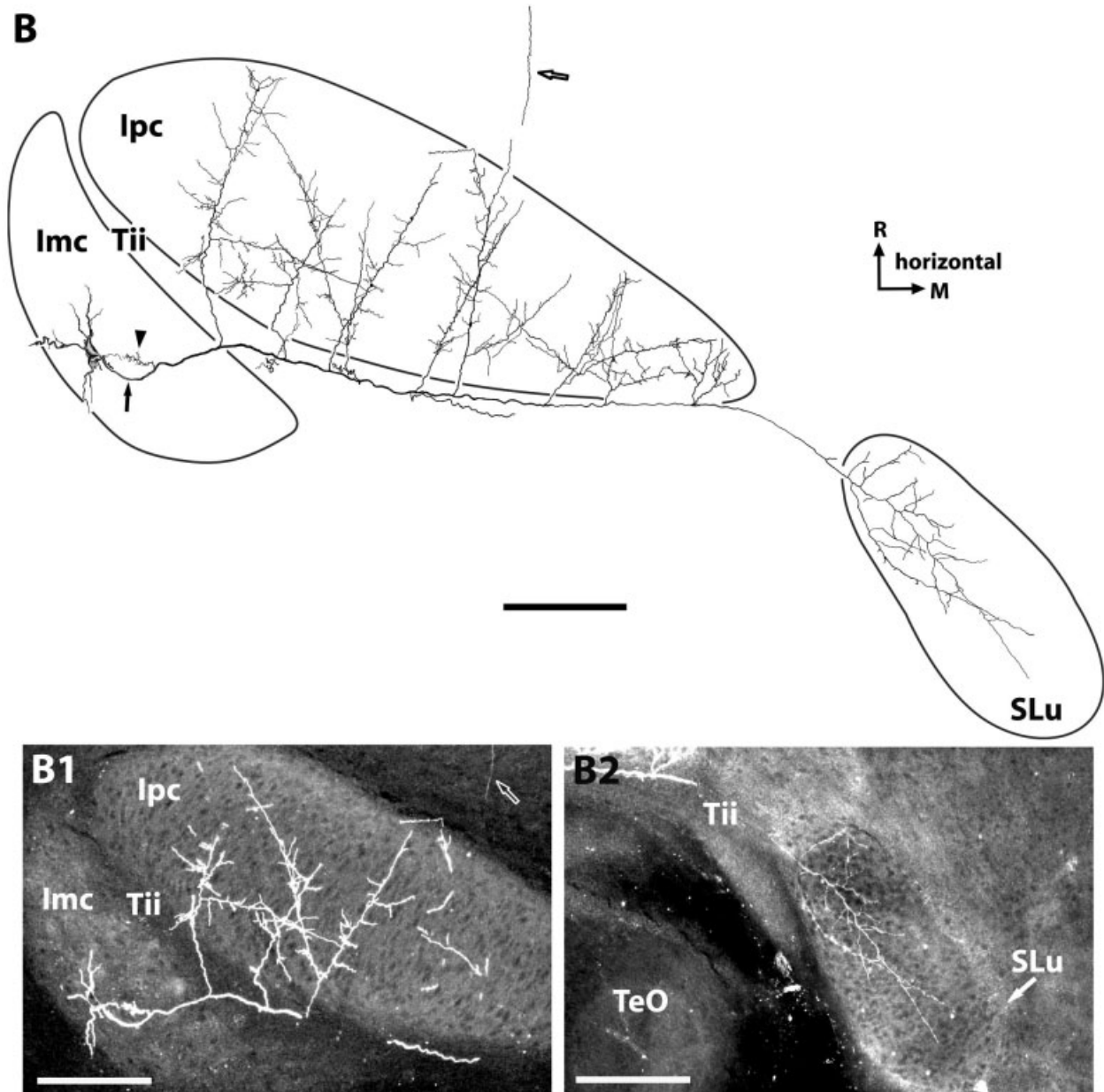
Figure 10 (Continued)

destinations. The rostrally directed branches shown in Figures 10B,C and 11C were noted above. In the neuron illustrated in Figure 12A, axon collaterals coursed laterally and caudally toward the TeO (arrowheads, Fig. 12A) while another collateral passed Ipc and coursed rostrally (arrow, Fig. 12A). The neuron shown in Figure 12B displayed a collateral coursing laterally toward the TeO (arrowhead, Fig. 12B), whereas another collateral (arrow, Fig. 12B) looped rostrally and medially around Ipc and gave one small branch into Ipc.

Local axonal collaterals. Some Imc neurons generated local axonal collaterals laden with terminal boutons. Some collateral arborizations were small (arrowheads, Fig. 10A,B), whereas others were more widely branching (open

arrow, Fig. 11C). Figure 13 illustrates a neuron located along the caudal margin of the Imc that gave rise to a widely branching axonal field. The main collaterals extended rostrolaterally and filled much of Imc with terminal branches, whereas the primary axon coursed into the Tii and left the parent slice medially.

Two possible subtypes of Imc neurons. Neurons projecting upon Ipc may project upon SLu as well, but this is difficult to demonstrate reliably in slice preparations. Insofar as no individual Imc neuron was found to project upon both Ipc/SLu and the TeO, there may be at least two subtypes of Imc neurons. Neurons projecting upon Ipc/SLu are referred to as *Imc-Is* neurons, and neurons projecting upon the TeO are referred to as *Imc-Te* neurons.
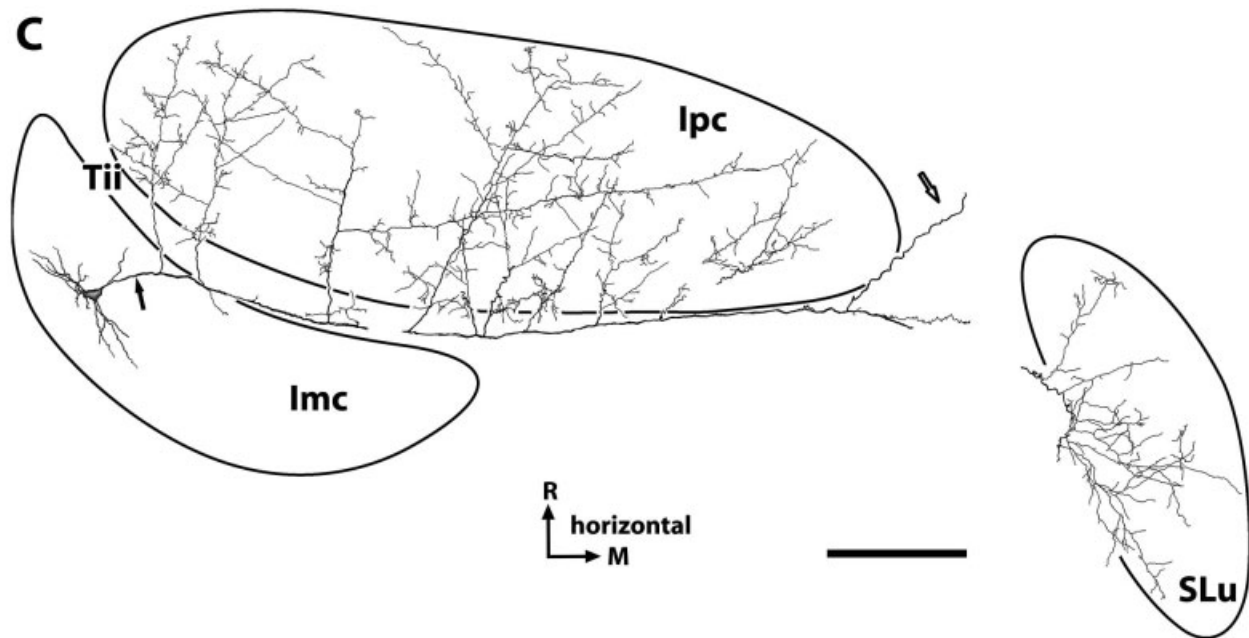
Figure 10.   (Continued)

Primary axons tend to emerge from the soma of the *Imc-Is* neurons and from a primary dendrite of the *Imc-Te* neurons (cf. Fig. 10 vs. Figs. 11, 12). The *Imc-Te* neurons usually possessed larger dendritic fields than the *Imc-Is* neurons (450–700 µm vs. 200–400 µm).

Peri-Imc neurons.   Figure 14 illustrates a neuron situated just outside the dorsal cytoarchitectonically defined boundary of Imc in a sagittal section. The spine-laden dendrites of this cell extended outside the boundary of Imc, without obvious penetration into the nucleus. The axon emerged from the base of a primary dendrite (solid arrow, Fig. 14), generated a wide local arborization, and extended caudoventrally into a widely ramifying terminal field in layers 10–13 (arrowheads, Fig. 14). Other collaterals coursed dorsally or rostrally toward an unknown target (open arrows, Fig. 14). One other comparable peri-Imc neuron was filled just outside the lateral boundary of Imc (not shown).

DISCUSSION

The isthmic region lies between the rostral rhombencephalon and the mesencephalon. The term originally referred to the narrow zone bridging these two major regions of the developing brainstem and was never intended to suggest a functional affiliation among the various nuclei of the so-called isthmic complex. The various isthmic nuclei are particularly well developed and differentiated in birds and consist of the ION, Imc, Ipc, and SLu. ION is the source of the major centrifugal projection upon the retina, and, although it also receives a projection from the TeO, it does not project back upon it and may not be directly involved in the functional circuitry of Imc, Ipc, and SLu.

Initially thought to be part of the auditory system, the isthmic complex is now recognized as a component of the visual system in all vertebrates (Wang, 2003). Some investigators have suggested that the physical separation of the isthmic complex from the TeO is related to some other, as yet unidentified, set of inputs or a unique spatial organization. Ipc and SLu have been extensively studied (Ramón y Cajal, 1911; Brecha, 1978; Güntürkün and Remy, 1990; Hellmann et al., 2001), and much attention has been devoted to explaining their reciprocal and precisely retinotopic connections with the TeO. For various technical reasons, the organization and connections of Imc have proved to be less readily distinguished, and the Imc's functional contribution has remained unclear.

The results of the current anatomical study suggest that the Imc does not function independently of, or in parallel with, Ipc/SLu. To the contrary, Imc fills a unique functional role vital to the function of the other components of the isthmic complex as well as the TeO. The nature of this contribution is illustrated by comparing the distinct patterns of connections, cell types, and both neurochemical and physiological features of the isthmic nuclei. The current study provides a more complete picture not only of the Imc but of the whole isthmotectal circuitry and its relationship with other information-processing streams of the TeO. Specific attention is paid to the relationship of the isthmotectal pathway to the motion-detection tectorotundal pathway.

Hodological topography

The various efferent pathways of the TeO differ in how they preserve retinotopy. The prominent TeO-rotundal projection lacks obvious retinotopy (see Marín et al., 2003), whereas the TeO-Ipc and TeO-Imc projection preserves a high degree of retinotopy. The Ipc-TeO projection is also highly retinotopic, such that corresponding points of the visual field representation in these two structures are reciprocally connected. The Imc-TeO projection, however, displays a unique organization. Imc neurons project
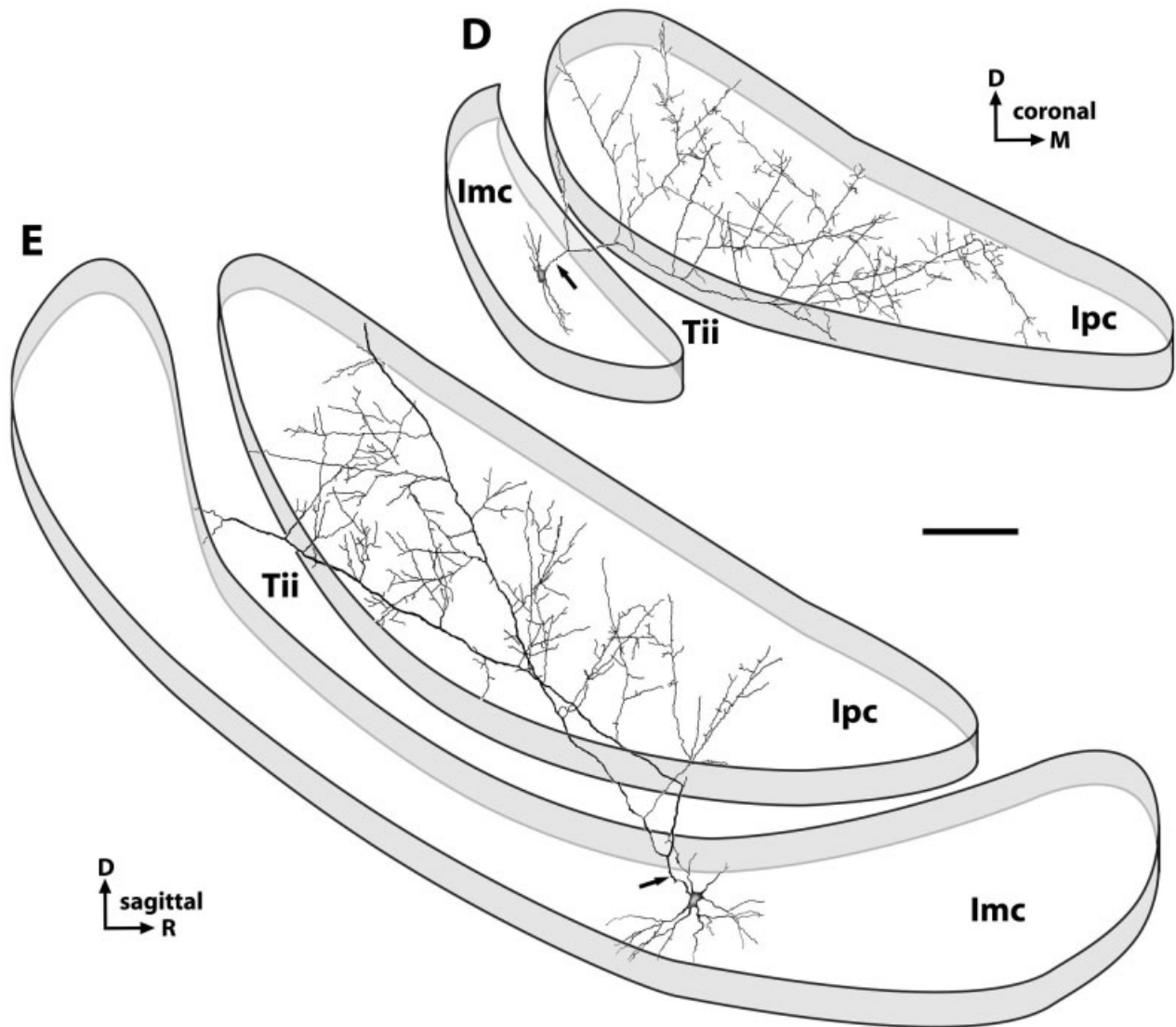
Figure 10   (Continued)

diffusely upon TeO but not to the locus from which they receive input. Whereas the TeO-Ipc-TeO pathway displays a *homotopic* reciprocal organization, the TeO-Imc-TeO pathway displays a *heterotopic* reciprocal organization. The current study does not identify a retinotopic organization in the projection from Imc upon Ipc/SLu. These hodological distinctions are summarized in Figure 15.

Two subtypes of Imc neurons

Imc neurons have multipolar somata that vary in size but have similar somatodendritic morphologies (see Güntürkün, 1987; Tömböl and Németh, 1998). The current study has further clarified that distal dendrites arborize within or along the margin of Imc and give rise to large, flattened dendritic fields. These dendritic fields are parallel to the long axes of Imc and approximately perpendicular to the columnar dendritic fields of Ipc neurons (Güntürkün, 1987). Tömböl and Németh (1998) divided Imc

neurons into "giant cells" and "large cells" on the basis of soma size and shape. The small sample of neurons in the current study does not convincingly demonstrate such a distinction. However, two subtypes of Imc neurons may be distinguished in terms of their axonal projections.

Imc-Is neurons (cell a, Fig. 15A) form extensive axonal arborizations throughout Ipc or both Ipc and SLu. They were the most commonly filled neuronal type, and their projection pattern suggests a coarse or nontopographic projection. Small injections of BDA into Ipc consistently labeled many neurons throughout Imc, supporting the conclusion that Imc-Is neurons constitute the majority of Imc neurons and that they project widely upon Ipc/SLu with overlapping terminal fields. Hodos and Karten (1974) suggested that Ipc was a major target of Imc, since retrogradely degenerating Imc neurons were observed following lesions of Ipc. This suggestion was confirmed by Tömböl et al. (1995), who reported fibers from Imc directed
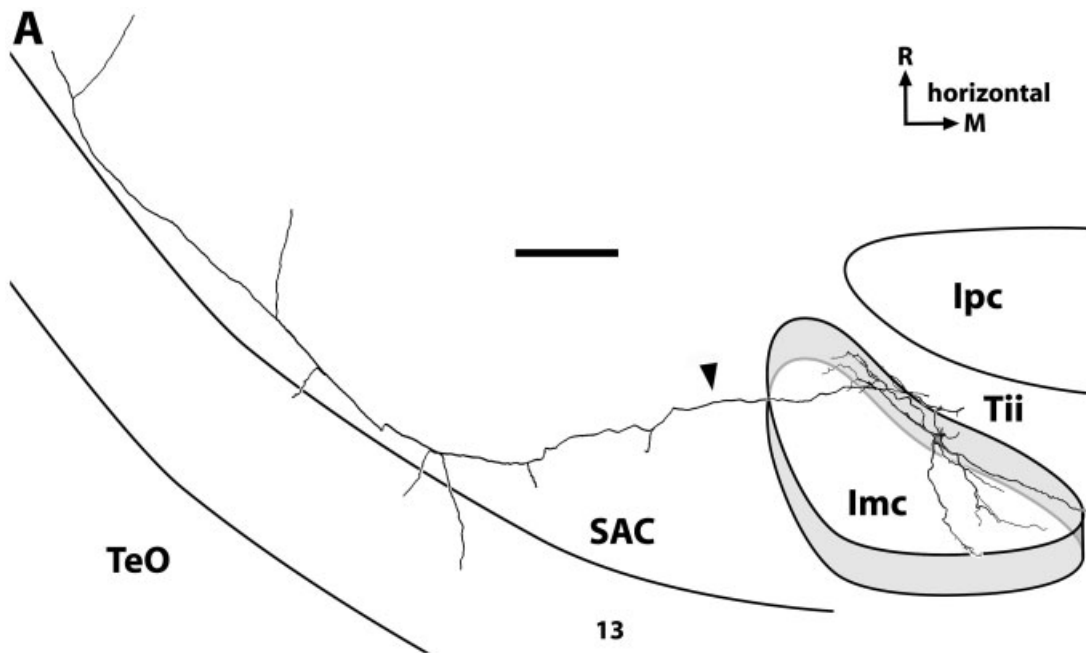
Fig. 11. Camera lucida reconstructions and photomicrographs of Imc neurons projecting upon the TeO. **A:** A horizontally sectioned Imc neuron that is situated along the medial side of Imc and projects upon a large field of the TeO. The primary axon (arrowhead) courses along the SAC and gives off several collaterals entering layer 13, where they fade away. **B:** A sagittally sectioned Imc neuron with a wide axonal ramifications within tectal layers 10–14. The primary axon emerges from a primary dendrite. **B1:** Darkfield image of the section contain- ing the ramifications within the TeO. **B2:** Nomarski-DIC images of fine, distal axonal branches within layers 10–12. **C:** A horizontally sectioned Imc neuron projecting upon tectal layers 10–14 (arrow- head). Other lateral and rostral collaterals course to unknown targets (solid arrows). This neuron gives off widely local branching processes within Imc (open arrow). Scale bars = 200 μm in A,B,B1,C, 25 μm in B2.

toward Ipc. The current study provides the first descrip- tion of the topography of the Imc-Ipc pathway. The cur- rent study also demonstrates with horizontal sections that individual Imc neurons project upon both Ipc and SLu. The projection to SLu may be similarly organized. How- ever, filling neurons in slice preparations may fail to re- veal subtle or small but clearly defined variations in ter- minal field density. Although a single Imc axon arborizes widely, it may not necessarily contact every neuron in Ipc/SLu. An alternate organization of this projection may exist, in which individual Imc neuron projects upon the whole area of Ipc/SLu, except for a small, selected region of interest, such as the region receiving the same tectal input source as that particular Imc neuron (see Fig. 15C).

Imc-Te neurons (cell b, Fig. 15A) project widely upon TeO with fine-caliber axonal fields. They were less fre- quently filled in intracellular studies. Injections of CTB in TeO retrogradely labeled a sparse population of Imc neu- rons that appeared to project widely upon TeO but prob- ably not to the loci of their tectal input. This heterotopic organization has also been observed in studies of the pi- geon (Y. Wang, unpublished observation). Imc-Te neurons may represent this sparse population of neurons with projections widely upon the TeO.

Brecha's (1978) study in pigeons correctly suggested that Imc axonal collaterals ramify within tectal layers 12–14. In addition, the current study reveals more super- ficial, wide ramifications within layers 10–11. Tömböl and her colleagues (Tömböl et al., 1995; Tömböl, 1998; Tömböl and Németh, 1998) suggested that Imc neurons possess large columnar terminal arborizations extending from tec- tal layer 2 to tectal layer 10 or 11. However, they did not visualize individual Imc neurons and their tectal termi- nals. Although columnar endings within TeO are observed after BDA injections into Imc, these could be attributed to labeling of fibers from Ipc passing through Imc.

Neurotransmitters in Imc efferent system

GABA appears to be a major neurotransmitter used by Imc neurons. The neuropils of Ipc and SLu express both GAD- and GABA-immunoreactive terminal boutons (Do- menici et al., 1988; Granda and Crossland, 1989; Veen- man and Reiner, 1994; Tömböl et al., 1995; Tömböl and Németh, 1998; Hellmann et al., 2001). Veenman et al. (1994) further reported that Ipc and SLu are rich in benzodiazepine-binding type $GABA_A$ receptors. Insofar as the somata of Ipc and SLu neurons are not GAD- immunoreactive or GABA-immunoreactive, Imc is the most likely source of GABAergic terminals (see Tömböl et al., 1995). Imc neurons are surrounded by scattered clus- ters of GAD-immunoreactive terminal boutons, which may derive from local axonal collaterals. Tectal layers 10–11 also contain GABAergic fibers (Granda and Cross- land, 1989). Wang et al. (1995b) reported that electrical stimulation of Imc excites tectal neurons in pigeons. This may be due to the activation of intrinsic inhibitory sys- tems within TeO and/or within Imc.

Although we could not confirm that all Imc neurons are GABA immunoreactive, none of the Imc neurons shows apparent ChAT immunoreactivity (Sorenson et al., 1989).
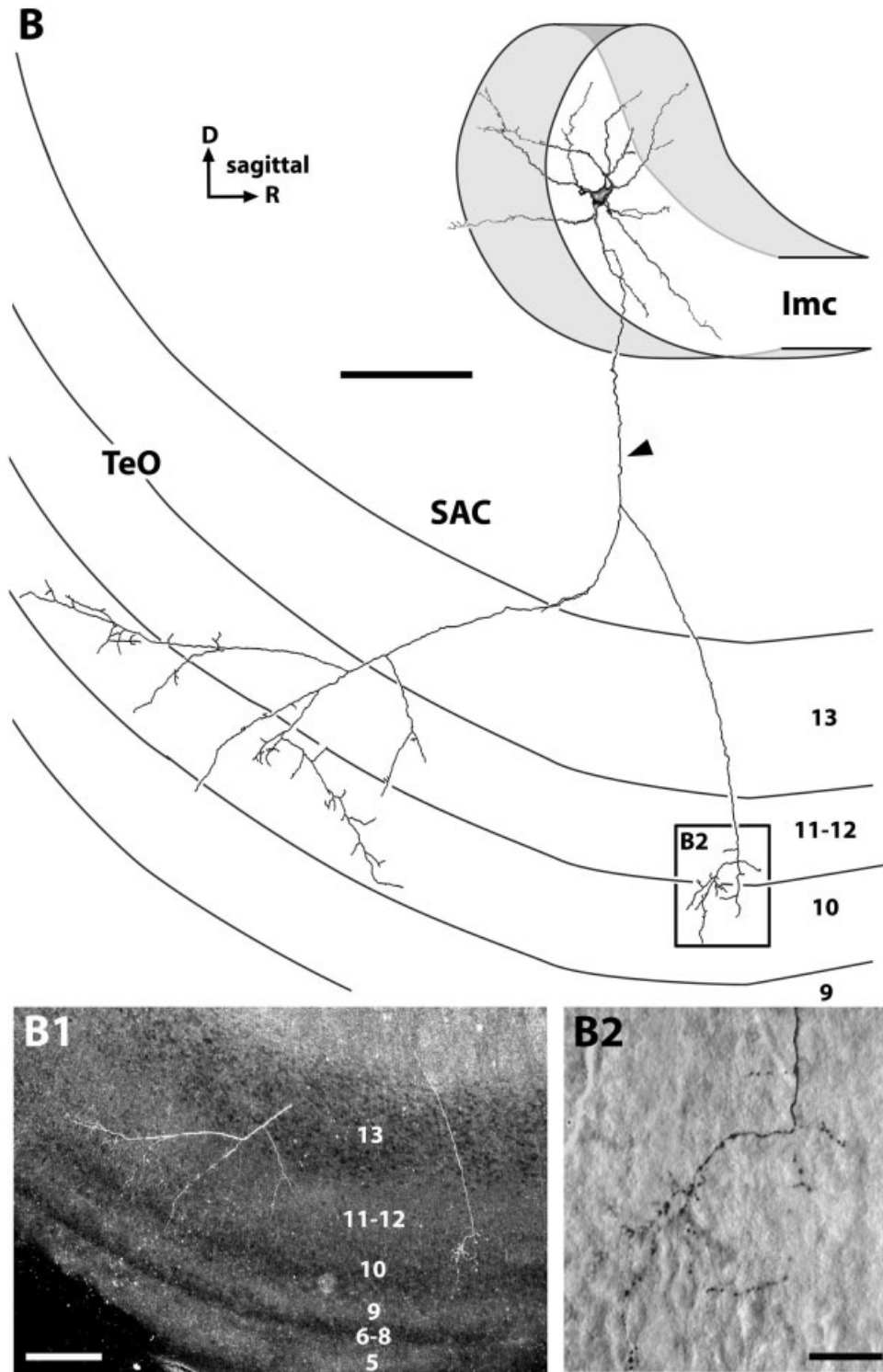
Figure 11 (Continued)

Imc neurons display intense AChE histochemical activity and issue the positive fibers in the Tii that project to Ipc and SLu. The function of AChE in Imc neurons remains unknown.

The projection of TeO upon Imc

The tectal cells projecting upon Imc proved difficult to distinguish from neurons projecting upon Ipc because of
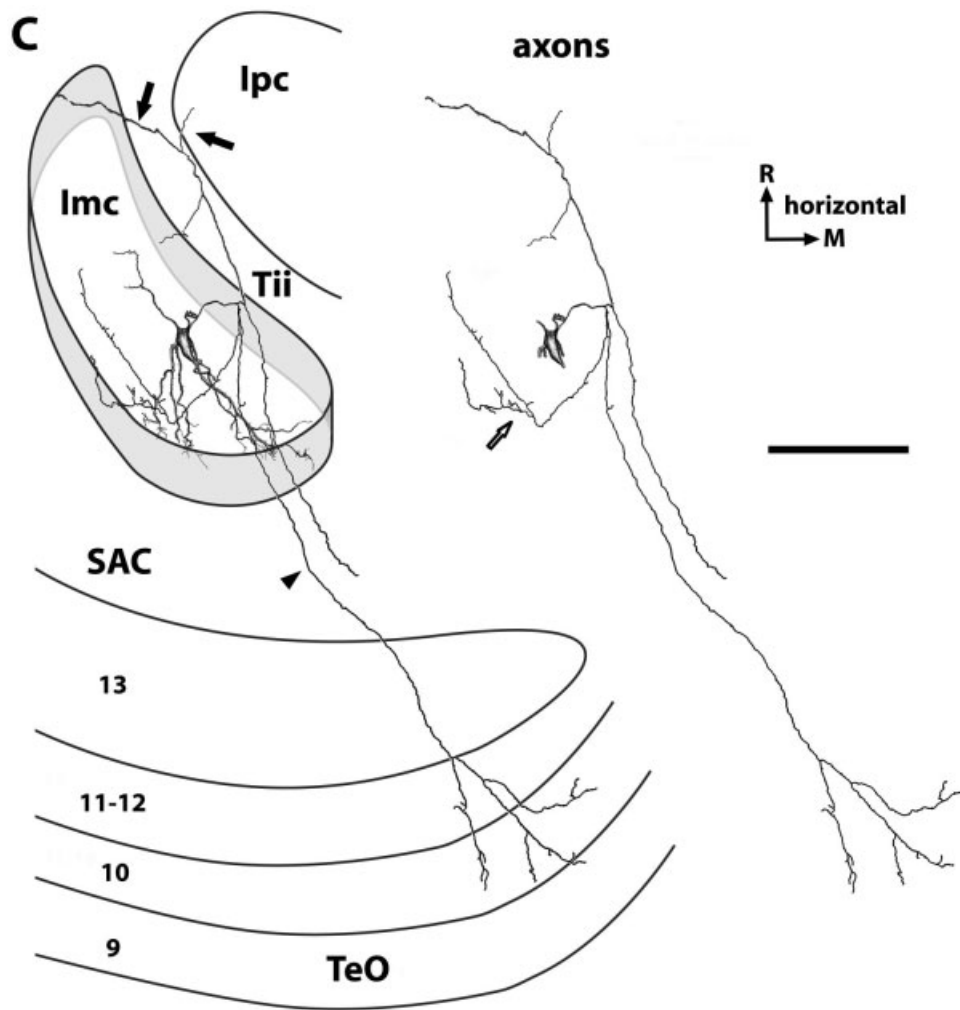
Figure 11   (Continued)

the likely labeling of passing fibers from the TeO upon Ipc (Ramón y Cajal, 1911; Hunt and Künzle, 1976; Y. Wang, unpublished observation). BDA injection into Imc in vitro retrogradely labeled radial neurons within layers 10–11. These neurons have "shepherd's crook" axons and dendritic arborizations within layers 5, 9, and 11, similar to the TeO-Ipc neurons identified in the current and previous retrograde tracing studies (Hunt et al., 1977; Woodson et al., 1991). The same type of tectal cells may project upon both Imc and Ipc. Individual tectal cells may issue axonal collaterals within Imc on their way to Ipc. Alternately, there maybe two different types of tectal cells, each projecting upon Imc and Ipc, respectively, although both types may possess "shepherd's crook" axons. In their Golgi study, Sebestény et al. (2002) reported that another type of radial neuron in layers 10–11 projects upon Imc. This type of neuron possesses dendritic side branches in layer 7, and its axon usually arises from the deep pole of the soma. This type of radial neuron was not visualized in our in vitro tracing experiments. Although in vitro tracing studies could not unambiguously identify the TeO-Imc

neurons, they showed that radial tectal neurons and their projections upon Imc and/or Ipc could be included within 500-μm-thick slices. Intracellular filling may be required in order to identify tectal cell types projecting upon the isthmic complex.

Functional implications

The functional roles of the isthmic complex remain enigmatic. The presence of a projection to the contralateral TeO in some vertebrates prompted the notion that the isthmic complex plays a role in tectally modulated stereopsis (see Wiggers and Roth, 1991). Martínez and Puelles (1989) reported the presence of sparse contralateral retrogradely labeled cells in a region that they suggested might be nucleus isthmi ventralis in chicks. However, the region of labeled cells that they illustrated may lie within the ventrocaudal margin of the lentiform nuclear complex rather than in the traditionally defined isthmic complex.

Physiological studies demonstrate that Imc and Ipc influence the center-surround organization of tectal neurons (S.R. Wang et al., 1995a; Y. Wang et al., 2000). Although interneurons within the TeO could provide the anatomical
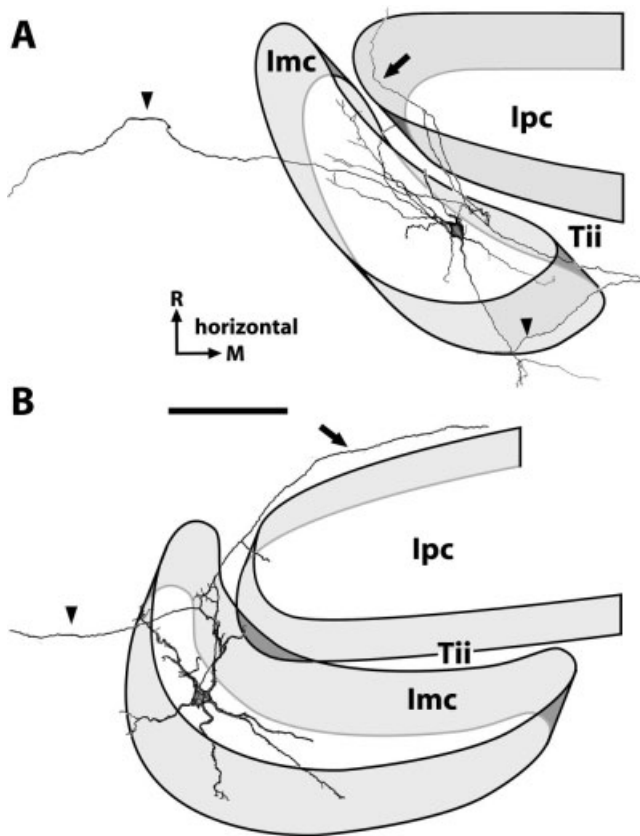
Fig. 12. Camera lucida reconstructions of horizontally sectioned Imc neurons that project upon the TeO and an unknown target. **A:** An Imc neuron that is situated along the medial side of the nucleus. Axonal collaterals (arrowheads) head toward the TeO, whereas another collateral (arrow) passes Ipc and courses rostrally before extending beyond the parent slice. **B:** An Imc neuron that possesses a similar axonal collateral coursing toward the TeO. Another collateral (arrow) loops along the lateral side of Ipc and courses rostromedially, with a branch entering Ipc. Scale bar = 200 μm.

Fig. 13. Camera lucida reconstruction of an Imc neuron with a wide, local axonal arborization that covers most of Imc itself. The soma gives off dendrites inward. The arrow indicates the primary axon. Scale bar = 200 μm.

substrate for this interaction, Imc provides an extensive, diffuse feed-forward projection upon Ipc/SLu and a diffuse, possibly heterotopic feedback projection upon the TeO. Ipc and Imc are likely to interact in a complex, dynamic manner in modulating receptive field properties. "Winner-take-all" (WTA) networks are one class of dynamic models that utilize center-surround interactions for visual target or attentional selection (Sereno and Ulinski, 1987; Y.C. Wang and Frost, 1991; S.R. Wang, 2003; for details on WTA networks see Feldman, 1982; Feldman and Ballard, 1982; Koch and Ullman, 1985).

One may speculate that, by virtue of its precise laminar and columnar patterns of connections within the TeO, the isthmic circuitry influences other tectal circuits organized in layers and columns. The avian tectorotundal pathway arising from layer 13 (SGC) represents one such system. SGC neurons (tectal ganglion neurons) generate large, monostratified arrays of small, columnar dendritic endings. In the revised nomenclature of Marín et al. (2003), dendritic endings of type I SGC neurons are stratified in retinorecipient tectal layers 5a–b (Luksch et al., 1998) and probably layer 3 (Brzozowska-Prechtl and Karten,
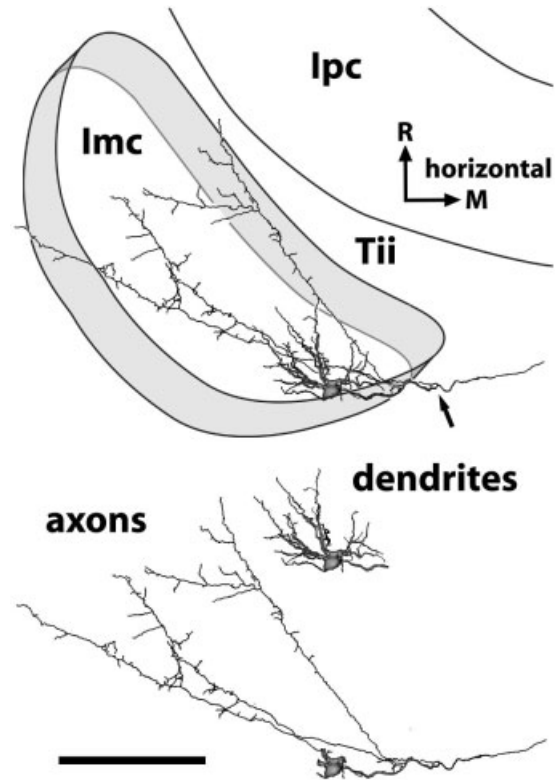
personal communication), whereas type II neurons have endings stratified in deeper nonretinorecipient layers 9–10 (see Fig. 15B). The paintbrush endings of Ipc and SLu neurons terminate within layers 2–7 (Ramón Y Cajal, 1911; Hunt et al., 1977; Brecha, 1978; Tömböl et al., 1995) and layers 6–13 (Brecha, 1978), respectively. Ipc and SLu terminals may thereby contact dendritic endings of type I (5a, 5b, and 3) and type II (9) SGC neurons, respectively. Neighboring bottlebrush endings of individual SGC neurons are approximately 50–70 μm apart (Luksch et al., 1998). Individual paintbrush endings of Ipc neurons are about 50 μm wide. Hence, a single paintbrush ending from Ipc and SLu may contact a single dendritic ending from one SGC neuron but numerous endings from different SGC neurons sampling the same columnar domain.

The dendritic organization of SGC neurons supports several of their more robust features: large receptive fields; sensitivity to small, moving stimuli; and unique "chattering" pattern of discharge (Luksch et al., 1998, 2001). Columnar terminals from the isthmic nuclei may serve to modulate correlated activity in multiple SGC cells sampling the same columnar domain (visual field locus). Widely spreading terminals provide a route for center-surround interactions. Taken together, these terminal patterns may modulate not only the classical receptive field of whole SGC cells but the activity of dendritic subdomains within single SGC cells. Such interactions could dynamically modulate a variety of motion-detection pa-
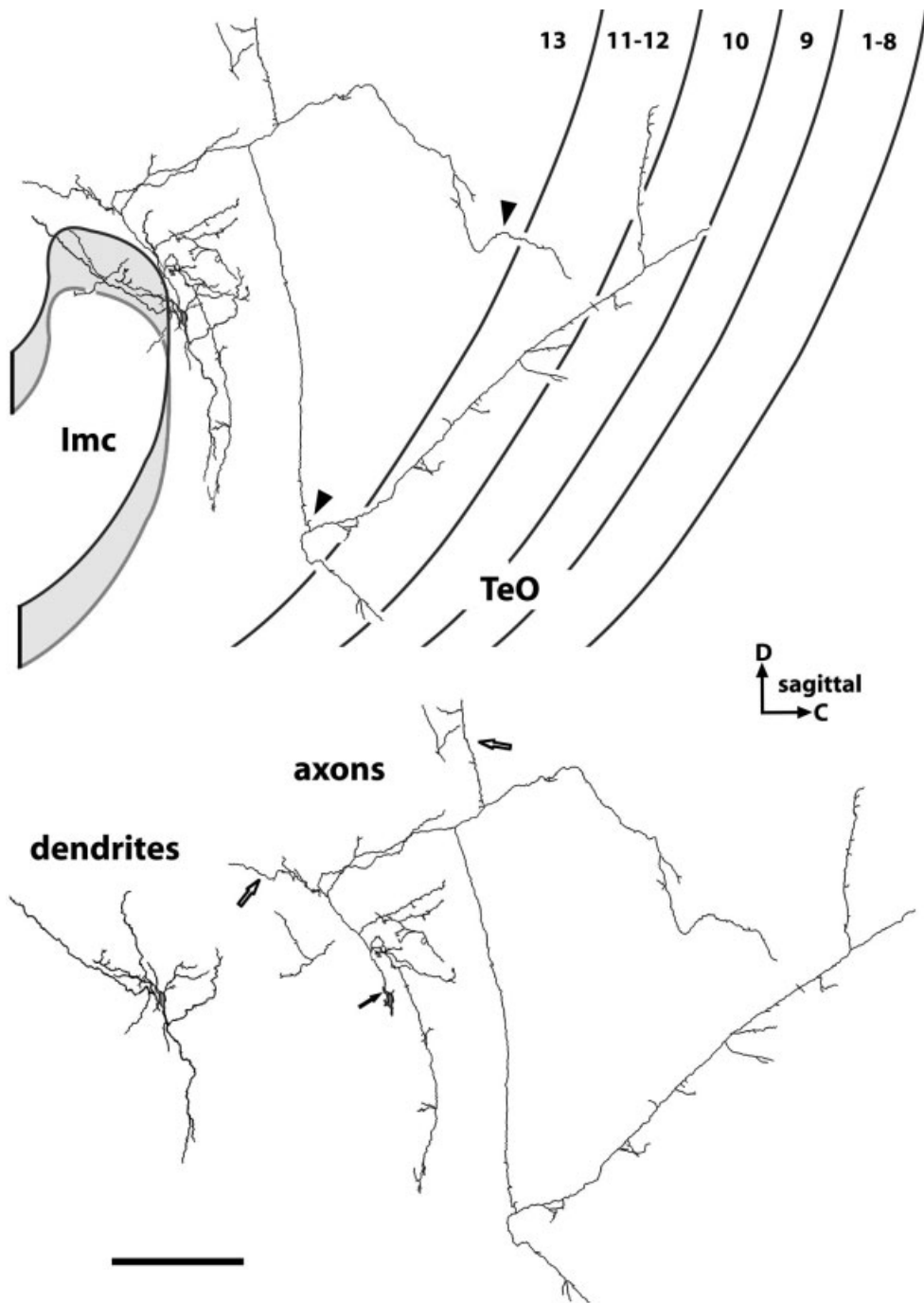
Fig. 14.   Camera lucida reconstruction of a peri-Imc neuron. See text for details. Scale bar = 200 μm.

rameters beyond that of global receptive field dimensions. Furthermore, given that distinct subtypes of SGC neurons project upon functionally distinct subdivisions of the nucleus rotundus (Karten et al., 1997; Hellmann and Güntürkün, 2001; Marín et al., 2003), the isthmic circuitry provides an early stage of interaction across information-processing streams.

Comparison with other vertebrates

Understanding the functional and evolutionary roles of the isthmic complex requires consideration and study of homologous systems in other vertebrates. The isthmic complex or comparable tegmental nuclei has been studied in various reptiles, amphibians, and fishes, although some of the most detailed studies have been pursued in turtles (Ser-
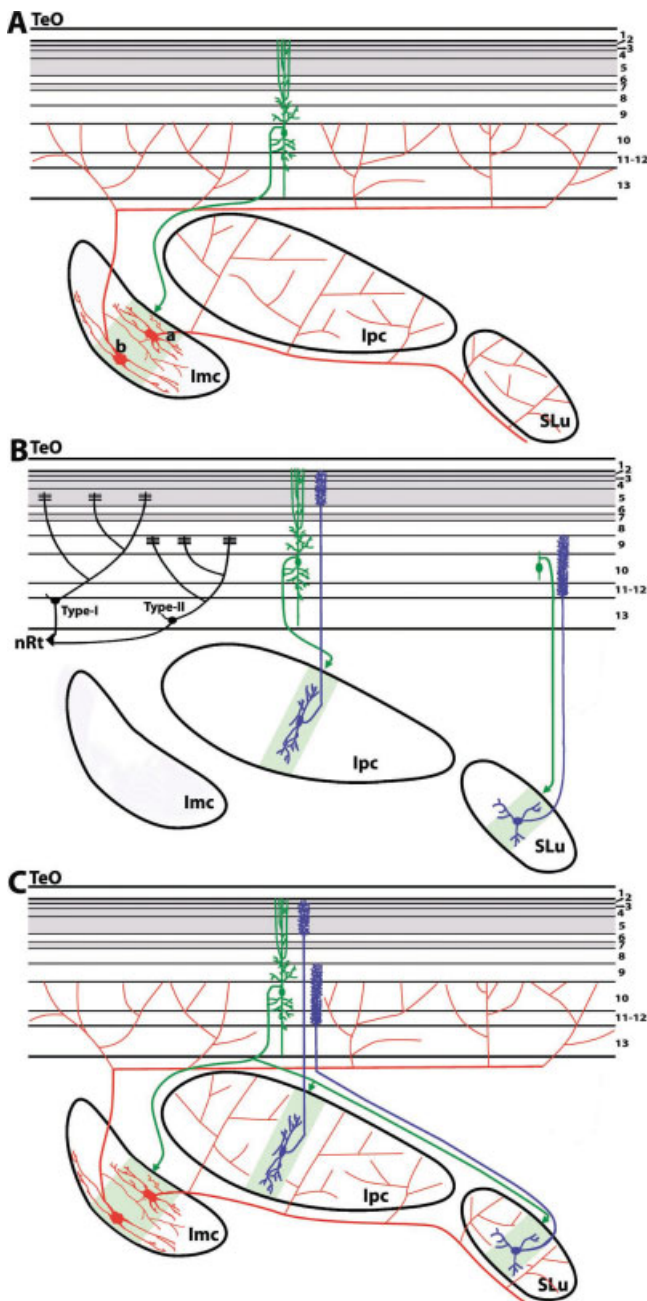
Fig. 15. Schematic drawings of the neuronal circuitry of the TeO, Imc, Ipc, and SLu. **A:** Imc receives a coarse topographical input from the radial tectal neurons in layers 10–11. Imc-Is neurons (a) and Imc-Te neurons (b) project widely upon Ipc/SLu and TeO, respectively. **B:** Ipc and SLu are retinotopically and reciprocally connected with the TeO. The paintbrush endings of Ipc and SLu neurons terminate within retinorecipient and nonretinorecipient tectal layers, respectively, ending in proximity to type I and type II SGC neurons (Luksch et al., 1998; Major et al., 2000; Morín et al., 2003). **C:** Summary of the intercircuitry among the TeO, Imc, Ipc, and SLu. The gray shadings of the TeO indicate retinorecipient tectal layers. The green shadings within Imc, Ipc, and SLu indicate the tectal terminal projection. The Ipc neuron is based on the reconstruction of an intracellular filled neuron (Y. Wang, unpublished observations). The SLu neuron is reproduced from Güntürkün's Golgi study (1987). nRt, nucleus rotundus. For other abbreviations see Figure 1 legend.

eno and Ulinksi, 1987). In mammals, the parabigeminal nucleus is considered the likely homologue of at least some component of the isthmic complex (Le Gros Clark, 1933).

Turtles. The cytoarchitecture, ipsilateral connections, and neurochemical features of the isthmic complex have striking similarities in birds (pigeons and chicks) and turtles (*Pseudemys scripta*). In the revised nomenclature of Powers and Reiner (1993), the isthmic complex in turtles consists of nucleus isthmi pars magnocellularis (Imc) and pars parvocellularis (Ipc), which were previously named *rostral* and *caudal magnocellular nucleus isthmi* (Sereno and Ulinski 1987). In the current paper, we adopt the nomenclature of Powers and Reiner (1993), which is consistent with the nomenclature in birds. After HRP injections into TeO, Sereno and Ulinski (1987) reported that Imc in turtles has wide, nontopographic, reciprocal connections with the ipsilateral TeO. Imc also projects nontopographically upon Ipc. Neurons of Imc have large, local axonal arborizations and long dendritic fields parallel to the long rostrocaudal axis of the nucleus. Imc contains GABAergic neurons (Powers and Reiner, 1993). The similarity between the avian Imc and the turtle Imc supports their proposed homology. As in the avian Ipc/SLu, the Ipc in turtles is reciprocally and topographically connected with the ipsilateral TeO. Terminals in the TeO consist of dense columnar arbors similar to the "paintbrush" endings in birds. The cells of Ipc are ChAT immunoreactive (Powers and Reiner, 1993).

Mammals. Abundant evidence indicates that the nucleus parabigeminalis (Pbg) of mammals is homologous to the Ipc/SLu complex of birds (Le Gros Clark, 1933; Künzle and Schnyder, 1984; Sereno and Ulinski, 1987; Diamond et al., 1992). Cells within the lateral tegmentum of mammals possess some features resembling the avian Imc (Sereno and Ulinski, 1987). The lateral tegmentum is just medial to Pbg, and many of its neurons are labeled following HRP injections into Pbg (Sherk, 1979). The neurons of the lateral tegmentum are GABAergic (Appell and Behan, 1990). The lateral tegmentum is reciprocally connected with the superior colliculus (Graybiel, 1978; Baleydier and Magnin, 1979; Roldan et al., 1983; Künzle and Schnyder, 1984). Jiang et al. (1996) further reported that the lateral tegmentum in the ferret projects to the superior colliculus in a less orderly fashion compared with Pbg. Roldan et al. (1983) reported that, in contrast to these observations regarding the lateral tegmentum, Pbg also provides a light, nontopographical projection upon the superior colliculus, suggesting that Pbg in mammals may combine feature of the avian Imc, Ipc, and SLu.

CONCLUSIONS

The historically obscure connections of Imc with Ipc, SLu, and TeO have been clarified in the current study. In contrast to the precise retinotopic connections of Ipc/SLu with TeO, Imc projects widely upon Ipc/SLu and upon TeO without obvious retinotopy. These two components of the isthmic complex likely exert dual effects on tectal neurons with regard to center-surround processing. Their columnar and laminar pattern of projections into the TeO may also support direct interactions with other information-processing streams, including the well-developed motion-processing tectorotundal pathway. Before any definitive statements can be made regarding the functional role of Imc, the precise synaptic organization and the activity of

neurotransmitters and receptors in this system have to be clarified. Studies in the highly differentiated avian visual system may be particularly useful for comparative studies with mammals, in which the isthmotectal system is less clearly distinguishable.

ACKNOWLEDGMENTS

LITERATURE CITED

Appell PP, Behan M. 1990. Sources of subcortical GABAergic projections to the superior colliculus in the cat. J Comp Neurol 302:143–158.

Ariëns Kappers CU, Huber GC, Crosby EC. 1960. The comparative anatomy of the nervous system of vertebrates, including man. New York: Hafner Publishing Co.

Baleydier C, Magnin M. 1979. Afferent and efferent connections of the parabigeminal nucleus in cat revealed by retrograde axonal transport of horseradish peroxidase. Brain Res 161:187–198.

Brecha N. 1978. Some observations on the organization of the avian optic tectum: afferent nuclei and their tectal projections. Thesis, State University of New York, Stony Brook.

Diamond IT, Fitzpatrick D, Conley M. 1992. A projection from the parabigeminal nucleus to the pulvinar nucleus in *Galago*. J Comp Neurol 316:375–382.

Domenici L, Waldvogel HJ, Matute C, Streit P. 1988. Distribution of GABA-like immunoreactivity in the pigeon brain. Neuroscience 25: 931–950.

Domesick VB, Morest DK. 1977. Migration and differentiation of shepherd's crook cells in the optic tectum of the chick embryo. Neuroscience 2:477–491.

Feldman JA. 1982. Dynamic connections in neural networks. Biol Cybern 46:27–39.

Feldman JA, Ballard DH. 1982. Connectionist models and their properties. Cogn Sci 6:205–254.

Granda RH, Crossland WJ. 1989. GABA-like immunoreactivity of neurons in the chicken diencephalon and mesencephalon. J Comp Neurol 287: 455–469.

Graybiel AM. 1978. A satellite system of the superior colliculus: the parabigeminal nucleus and its projections to the superficial collicular layers. Brain Res 145:365–374.

Güntürkün O. 1987. A Golgi study of the isthmic nuclei in the pigeon (*Columba livia*). Cell Tissue Res 248:439–448.

Güntürkün O, Remy M. 1990. The topographical projection of the nucleus isthmi pars parvocellularis (Ipc) onto the tectum opticum in the pigeon. Neurosci Lett 111:18–22.

Hellmann B, Güntürkün O. 2001. Structural organization of parallel information processing within the tectofugal visual system of the pigeon. J Comp Neurol 429:94–112.

Hellmann B, Manns M, Güntürkün O. 2001. Nucleus isthmi, pars semilunaris as a key component of the tectofugal visual system in pigeons. J Comp Neurol 436:153–166.

Hodos W, Karten HJ. 1974. Visual intensity and pattern discrimination deficits after lesions of the optic lobes in pigeons. Brain Behav Evol 9:165–194.

Hunt SP, Künzle H. 1976. Observations on the projections and intrinsic organization of the pigeon optic tectum: an autoradiographic study based on anterograde and retrograde, axonal and dendritic flow. J Comp Neurol 170:153–172.

Hunt SP, Streit P, Künzle H, Cuénod M. 1977. Characterization of the pigeon isthmotectal pathway by selective uptake and retrograde movement of radioactive compounds and by Golgi-like horseradish peroxidase labeling. Brain Res 129:197–212.

Iñiguez C, Gayoso MJ, Carreres J. 1985. A versatile and simple method for staining nervous tissue using Giemsa dye. J Neurosci Methods 13:77–86.

Jiang ZD, King AJ, Moore DR. 1996. Topographic organization of projection from the parabigeminal nucleus to the superior colliculus in the

ferret revealed with fluorescent latex microspheres. Brain Res 743: 217–232.

Karten HJ. 1967. The organization of the ascending auditory pathway in the pigeon (*Columba livia*). I. Diencephalic projections of the inferior colliculus (nucleus mesencephali lateralis, pars dorsalis). Brain Res 6:409–427.

Karten HJ, Cox K, Mpodozis J. 1997. Two distinct populations of tectal neurons have unique connections within the retinotectorotundal pathway of the pigeon (*Columba livia*). J Comp Neurol 387:449–465.

Katz DM, Karten HJ. 1983. Subnuclear organization of the dorsal motor nucleus of the vagus nerve in the pigeon, *Columbia livia*. J Comp Neurol 217:31–46.

Koch C, Ullman S. 1985. Shifts in selective visual attention: towards the underlying neural circuitry. Hum Neurobiol 4:219–227.

Künzle H, Schnyder H. 1984. The isthmus-tegmentum complex in the turtle and rat: a comparative analysis of its interconnections with the optic tectum. Exp Brain Res 56:509–522.

Le Gros Clark WE. 1933. The medial geniculate body and the nucleus isthmi. J Anat 67:536–548.

Luksch H, Cox K, Karten HJ. 1998. Bottlebrush dendritic endings and large dendritic fields: motion-detecting neurons in the tectofugal pathway. J Comp Neurol 396:399–414.

Luksch H, Karten HJ, Kleinfeld D, Wessel R. 2001. Chattering and differential signal processing in identified motion-sensitive neurons of parallel visual pathways in the chick tectum. J Neurosci 21:6440–6446.

Major DE, Luksch H, Karten HJ. 2000. Bottlebrush dendritic endings and large dendritic fields: motion-detecting neurons in the mammalian tectum. J Comp Neurol 423:243–260.

Marín G, Letelier JC, Henny P, Sentis E, Farfán G, Fredes F, Pohl N, Karten HJ, Mpodozis J. 2003. Spatial organization of the pigeon tectorotundal pathway: an interdigitating topographic arrangement. J Comp Neurol 458:361–380.

Martínez S, Puelles L. 1989. Avian nucleus isthmi ventralis projects to the contralateral optic tectum. Brain Res 481:181–184.

McGill JI, Powell TP, Cowan WM. 1966. The organization of the projection of the centrifugal fibers to the retina in the pigeon. J Anat 100:35–49.

Medina L, Reiner A. 1994. Distribution of choline acetyltransferase immunoreactivity in the pigeon brain. J Comp Neurol 342:497–537.

Mpodozis J, Cox K, Shimizu T, Bischof HJ, Woodson W, Karten HJ. 1996. GABAergic inputs to the nucleus rotundus (pulvinar inferior) of the pigeon (*Columba livia*). J Comp Neurol 374:204–222.

Palmgren A. 1921. Embryological and morphological studies on the midbrain and cerebellum of vertebrates. Acta Zool 2:1–94.

Powers AS, Reiner A. 1993. The distribution of cholinergic neurons in the central nervous system of turtles. Brain Behav Evol 41:326–345.

Ramón y Cajal S. 1911. Histologie du système nerveux de l'homme et des vertébrés. Translated by L. Azoulay. Paris: Maloine.

Rodman HR, Karten HJ. 1995. Laminar distribution and sources of catecholaminergic input to the optic tectum of the pigeon (*Columba livia*). J Comp Neurol 359:424–442.

Roldan M, Reinoso-Suarez F, Tortelly A. 1983. Parabigeminal projections to the superior colliculus in the cat. Brain Res 280:1–13.

Sebestény T, Davies DC, Zayats N, Németh A, Tömböl T. 2002. The ramification and connections of retinal fibres in layer 7 of the domestic chick optic tectum: a Golgi impregnation, anterograde tracer and GABA-immunogold study. J Anat 200:169–183.

Sereno MI, Ulinski PS. 1987. Caudal topographic nucleus isthmi and the rostral nontopographic nucleus isthmi in the turtle, *Pseudemys scripta*. J Comp Neurol 261:319–346.

Sherk H. 1979. Connections and visual-field mapping in cat's tectoparabigeminal circuit. J Neurophysiol 42:1656–1668.

Shimizu T, Cox K, Karten HJ, Britto LRG. 1994. Cholera toxin mapping of retinal projections in pigeons (*Columba livia*), with emphasis on retinohypothalamic connections. Vis Neurosci 11:441–446.

Showers MJC, Lyons P. 1968. Avian nucleus isthmi and its relation to hippus. J Comp Neurol 132:589–616.

Sorenson EM, Parkinson D, Dahl JL, Chiappinelli VA. 1989. Immunohistochemical localization of choline acetyltransferase in the chicken mesencephalon. J Comp Neurol 281:641–657.

Tömböl T. 1998. Golgi and electron-microscopic Golgi-GABA immunostaining study of the avian optic tectum. Acta Anat 162:209–225.

Tömböl T, Németh A. 1998. GABA-immunohistological observations, at the electron-microscopical level, of the neurons of isthmi nuclei in chicken, *Gallus domesticus*. Cell Tissue Res 291:255–266.

Tömböl T, Egedi GY, Németh A. 1995. Some data on connections of neurons of nuclei isthmi of the chicken. J Hirnforsch 36:501–508.

Uchiyama H. 1989. Centrifugal pathways to the retina: influence of the optic tectum. Vis Neurosci 3:183–206.

Vaage S. 1973. The histogenesis of the isthmic nuclei in chick embryos (*Gallus domesticus*). I. A morphological study. Z Anat Entwicklungsgesch 142:283–314.

Veenman CL, Reiner A. 1994. The distribution of GABA-containing perikarya, fibers and terminals in the forebrain and midbrain of pigeons, with particular reference to the basal ganglia and its projection targets. J Comp Neurol 339:209–250.

Veenman CL, Albin RL, Richfield EK, Reiner A. 1994. Distributions of $GABA_A$, $GABA_B$, and benzodiazepine receptors in the forebrain and midbrain of pigeons. J Comp Neurol 344:161–189.

Wang SR. 2003. The nucleus isthmi and dual modulation of the receptive field of tectal neurons in non-mammals. Brain Res Brain Res Rev 41:13–25.

Wang SR, Wang YC, Frost BJ. 1995a. Magnocellular and parvocellular divisions of pigeon nucleus isthmi differentially modulate visual responses in the tectum. Exp Brain Res 104:376–384.

Wang SR, Wu GY, Felix D. 1995b. Avian Imc-tectal projection is mediated by acetylcholine and glutamate. Neuroreport 6:757–760.

Wang Y, Xiao J, Wang SR. 2000. Excitatory and inhibitory receptive fields of tectal cells are differentially modified by magnocellular and parvocellular divisions of the pigeon nucleus isthmi. J Comp Physiol A186:505–511.

Wang YC, Frost BJ. 1991. Visual response characteristics of neurons in the nucleus isthmi magnocellularis and nucleus isthmi parvocellularis of pigeons. Exp Brain Res 87:624–633.

Wiggers W, Roth G. 1991. Anatomy, neurophysiology and functional aspects of the nucleus isthmi in salamanders of the family Plethodontidae. J Comp Physiol 169:165–176.

Woodson W, Reiner A, Anderson K, Karten HJ. 1991. Distribution, laminar location, and morphology of tectal neurons projecting to the isthmo-optic nucleus and the nucleus isthmi, pars parvocellularis in the pigeon (*Columba livia*) and chick (*Gallus domesticus*): a retrograde labeling study. J Comp Neurol 305:470–488.

Woodson W, Shimizu T, Wild JM, Schimke J, Cox K, Karten HJ. 1995. Centrifugal projections upon the retina: an anterograde tracing study in the pigeon (*Columba livia*). J Comp Neurol 362:489–509.